Compositional variation of the Zechstein Group in the Norwegian North Sea: implications for underground storage in salt caverns

Dora Marín (corresponding author)
Vår Energi,
Vestre Svanholmen 1,
Sandnes, Norway
doraluzmr@gmail.com

Néstor Cardozo
Professor of Structural geology
Department of Energy Resources
University of Stavanger
4036 Stavanger
Norway
nestor.cardozo@uis.no

Alejandro Escalona
Head, Department of Energy Resources
Department of Energy Resources
University of Stavanger
4036 Stavanger
Norway
alejandro.escalona@uis.no

Compositional variation of the Zechstein Group in the Norwegian North Sea: implications for underground storage in salt caverns

Dora Marín[1], Néstor Cardozo[2], Alejandro Escalona[2]

1 Vår Energi, Norway

2 Department of Energy Resources, University of Stavanger

Abstract

Halite beds in the upper Permian Zechstein Group represent an opportunity for the future development of underground storage caverns. However, geologic factors such as lithological heterogeneities, cap rock characteristics, and depth can affect the sealing capacity and the integrity of the cavern or contaminate the stored fluid. The main objective of this paper is to evaluate these factors focusing on the compositional variation of the Zechstein Group in different salt structures in the Norwegian North Sea, and related opportunities and challenges for salt cavern storage. Based on deformation style, geometry, height, and thickness of the salt structures, we have divided the Zechstein Group into four main categories: 1) thin beds, which can be either carbonate-anhydrite or clastic dominated. Halite is absent and therefore there is no potential for the development of salt caverns. 2 and 3) bedded to weakly deformed evaporites and intermediate size salt structures, where thick halite beds of more than 300 m are present, but they are usually deeper than 2000 m. Lithological heterogeneities in the halite consist of a mix of competent and incompetent (K-Mg salts) lithologies. 4) Tall diapirs, characterized by shallower structures (< 2000 m), with large deformation and poor seismic image. Thin layers of incompetent K-Mg salts are observed in these diapirs. The composition, thickness and deformation of the cap rock vary greatly in the area. Thick halite beds are recognized in most salt structures, suggesting an opportunity for underground storage. The challenges are related to the depth of the halite, amount and type of heterogeneities, characteristics of the cap rock, and deformation in the different salt structures. These results also have implications for the distribution of reservoir and source rocks, and the evolution of the Northern Permian Basin.

Key words: Zechstein Group, North Sea, salt caverns, underground storage

1. Introduction

Salt caverns are safe storage sites of varied energy carriers and waste due to the properties of halite: impermeability, high solubility, and low contamination rates (Koyi, 1991; Gillhaus and Horvath, 2008; Kruck et al., 2013; Crotogino, 2016; Tarkowski, 2019; Caglayan et al., 2020; Duffy et al., 2022; Allsop et al., 2023). Halite is the target for underground storage caverns. However, halite usually occurs as layered evaporitic sequences (LES) containing beds of different composition and mechanical properties such as different evaporites, carbonate, clastic and volcanic rocks (Warren, 2006; Raith et al., 2015; Strozyk et al., 2017; Rowan, et al., 2019). The proportion of these components control the

sealing properties, the contamination of the stored fluid, and the final geometry of the salt cavern (Gillhaus and Horvath, 2008; Hemme and van Berk, 2017; Looff, 2017; Cyran, 2020; Kumar et al., 2021; Portarapillo and Di Benedetto, 2021). The presence of ductile and low-viscosity K-Mg salts can be highly problematic during the drilling process, leading to project delays or well abandonment (Strozyk et al., 2017). LES deform in the subsurface, creating a wide variety of salt structures including bedded salt, pillows, anticlines, and diapirs (walls and stocks) (e.g., Gillhaus and Horvath, 2008; Jackson and Hudec, 2017). The prediction of lithological heterogeneities in the different salt structures is crucial to select the best cavern location and minimize drilling risks (Duffy et al., 2022). However, this is difficult to achieve because of often poor well control and seismic quality (Rowan, et al., 2019; Duffy et al., 2022).

The Norwegian North Sea (NNS) is an energy hub; thus, it is important to identify geological storage opportunities within salt caverns. This region is exceptional due to the large amount of publicly available subsurface data, which makes possible studying the compositional variation of LES of the Upper Permian Zechstein Group, (Figure 1). The Zechstein Group is not present in Norway mainland and therefore this study focuses offshore. Studies of the Zechstein Group in the NNS are mainly related to salt tectonics and suprasalt deformation (Kane et al., 2010; Lewis et al., 2013; Karlo et al., 2014; Jackson and Lewis, 2016; Jackson et al., 2018). The accepted interpretation is that salt tectonics in this area started during the Triassic (Sørensen et al., 1992; Smith et al., 1993; Karlo et al., 2014; Jackson et al., 2018). However, studies from the Dutch and UK sectors of the North Sea suggest that the Zechstein Group experienced syn-depositional deformation (Stewart, 2007; Pichat, 2022). Thus, it is unclear if the Zechstein Group is synkinematic in the Norwegian sector too. Jackson et al. (2019) describe the role of lithological variations in the Zechstein Group on the deformation style in the central part of the NNS. They conclude that thick mobile and thin immobile evaporites controlled the presence or absence of diapirism. Jackson and Lewis (2012) and Jackson and Lewis (2016) interpret the composition of the Zechstein Group in the northern part the Egersund Basin and the eastern Sele High. The focus of these studies is not underground storage caverns, therefore lithological heterogeneities, depth, geometry, and thickness of salt structures are briefly described.

Different types of salt structures have been identified in the NNS (e.g., salt walls, stocks, dendritic and irregular salt structures, collapsed anticlines, etc.) (Stewart, 2007; Karlo et al., 2014; Jackson and Hudec, 2017; Jackson and Stewart, 2017). Nevertheless, it is unclear if these different structures have different internal compositions. The main objective of this study is to describe the salt structures and compositional variations of the Zechstein Group in the NNS, to better understand the opportunities and challenges for salt cavern storage. We focus on the description of lithological heterogeneities within the Zechstein Group, the relationship between compositional variation and the type of salt structure, and the Zechstein Group syn-depositional deformation. The results of this study can contribute to better assess the risk of underground storage caverns projects in the Zechstein Group in Europe.

1.1 Geological storage in salt caverns

Salt caverns are built by water-driven halite dissolution (Kruck et al., 2013). Halite can be interbedded with minerals and rocks of lower solubility such as anhydrite, gypsum, carbonate, and clastic rocks, which can cause cavern shape anomalies (such as narrower zones) (Warren, 2006; Jackson and Hudec, 2017, Looff, 2017; Cyran, 2020). Some of these rocks have higher permeability and are more competent than halite, leading to fracture and fault development that affect the sealing quality of the cavern (Looff, 2017). This is particularly important for hydrogen storage, where the molecule is small

and mobile, and the risk of leakage is higher (Ozarslan, 2012). Furthermore, diapir boundaries and especially the crest, are exposed to halite dissolution by meteoric and formation water, and bacterial action, resulting in a carbonate, gypsum and anhydrite dominated zone called the cap rock (Posey and Kyle, 1998; Loof et al, 2003; Jackson and Hudec, 2017; Caesar et al., 2019). The cap rock can contain reservoir units due to its high permeability (Posey and Kyle, 1998; Jackson and Hudec, 2017). Thus, it is important to understand the thickness and characteristics of the cap rock for salt cavern location planning. Lithological heterogeneities can also stimulate the presence of bacteria contaminating the stored fluid (e.g., hydrogen or hydrocarbons), particularly at the bottom of the cavern, where the insoluble material is accumulated after the cavern construction (Kruck et al., 2013; Panfilov, 2016; Hemme and van Berk, 2017; Portarapillo and Di Benedetto, 2021). Other contaminating sources commonly present in LES are anhydrite or pyrite, which can act as sulfate sources (Reitenbach et al., 2015; Hemme and van Berk, 2017).

K-Mg salts are commonly present in LES. These minerals are more soluble than halite and enlarged cavern anomalies are usually formed when they are present (Warren, 2006; Jackson and Hudec, 2017; Loof, 2017). Creep can also affect the stability of salt caverns and lead to surface subsidence (Warren, 2006). Creep is accelerated by high temperature and pressure, the presence of K-Mg salts, fluid content, and a halite fine-grained size (Warren, 2006; Urai and Spiers, 2007; Jackson and Hudec, 2017; Loof, 2017). Most salt caverns are placed between few hundreds of meters to 2000 m, where they are generally stable (Warren, 2006; Gillhaus and Horvath, 2008). Depths shallower than 1500 m are preferred for compressed air salt caverns storage (Parkes et al., 2018). Salt cavern dimensions vary greatly, but commonly they are around 300 m high and 60 m wide (Gillhaus and Horvath, 2008; Caglayan et al., 2020).

2. Geological setting

2.1 Tectonic setting

During the Permian, northern Europe was characterized by two main basins: the northern and the southern Permian basins (Glennie and Underhill, 1998; Glennie et al., 2003). The study area was in the northern Permian Basin, which was affected by early Permian extension and strike-slip faulting (e.g., the Egersund Basin), following the Variscan orogeny collapse (Glennie and Underhill, 1998; Sørensen et al., 1992; Jackson and Lewis; 2013). Thermal subsidence, transtension, and normal faulting characterized the late Permian (Sørensen et al, 1992; Glennie and Underhill, 1998; Kalani et al., 2020). Tectonic activity during the deposition of the Zechstein Group (late Permian, Lopingian) is poorly constrained in the study area due to the mobile character of the evaporites (Jackson et al., 2019). Thickness and compositional variations in the Zechstein Group have been linked to the major faults of the NW part of the study area (Sørensen et al, 1992; Kalani et al., 2020; Jackson and Lewis, 2016; Jackson et al., 2019). However, it is uncertain whether these thickness variations result from post-depositional salt movement, syn-rift activity, or inherited relief (Jackson and Lewis, 2016; Jackson et al., 2019). The consensus is that salt tectonics started in the Triassic in the area, creating a great variety of salt structures (Figure 2b) (Sørensen et al., 1992; Smith et al., 1993; Karlo et al., 2014; Jackson et al., 2019). Some of these structures continued to grow during the rest of the Mesozoic and Cenozoic (Davison et al., 2000; Jackson and Stewart, 2017).

2.2 Stratigraphy

The Zechstein Group is a salt giant deposit in the southern and northern Permian basins (Taylor, 1998). The group has been divided into four main cycles, Z1-Z4 (though cycles Z5-Z6 are locally present), and

its base is marked by the thin, organic-rich claystone of the Kupferschiefer Formation (Figure 2a) (van Adrichem Boogaert and Kouwe, 1993; Taylor, 1998). Ideally, these cycles are composed of fine-grained clastic rocks at the base, followed by carbonates, anhydrite, halite, and K-Mg salts (van Adrichem Boogaert and Kouwe, 1993; Taylor, 1998). However, the Zechstein Group exhibits lateral variations. Carbonate and anhydrite were mainly deposited in the shallow basin margins; while thick halite packages with carnalite, anhydrite and claystone stringers characterize the depocenter (Sørensen et al., 1992; van Adrichem Boogaert and Kouwe, 1993; Clark et al., 1998; Taylor, 1998; Glennie et al., 2003; Sorento et al., 2018; Jackson et al., 2019; Pichat, 2022). Halite is particularly abundant in the second cycle Z2, which has been preferentially used for salt cavern construction in areas such as Germany, Poland, or the Netherlands, although caverns have also been built in lesser proportion in the other cycles (van Adrichem Boogaert and Kouwe, 1993; Taylor, 1998; Gillhaus and Horvath, 2008). The Zechstein cycles have not been formally recognized in the NNS, although there are great similarities with the other North European regions (Figure 2a). The Zechstein Group in the NNS has been penetrated by 138 wells, and the Kupferschiefer Formation is reported in 24 wells with a thickness of usually less than 3 m (NPD, 2022). Areas such as the segments of the Utsira High are interpreted as an upper Permian carbonate platform, where the Zechstein Group is thin and mainly composed of carbonates, clastic rocks, and anhydrite (Sorento et al., 2018; Jackson et al., 2019).

3. Methods

Subsurface data (3D and 2D seismic, well logs, cores, and reports) from the public Norwegian Petroleum Directorate (NPD) Diskos database covering an area of 42 000 km^2 were used in this study (Figure 1b). The western part is fully covered by 3D seismic, whereas other areas particularly the southeastern part contain scarce 2D seismic data (Figure 1b). The information of the 3D and 2D seismic surveys interpreted in this study are provided in supplementary material 1 and 2. Wells were used with different aims: First, wells that penetrate the Zechstein Group were used to constrain the seismic interpretation (Figure 1b, supplementary material 3). Second, well logs (gamma ray, sonic, density, neutron, and caliper) together with well reports (particularly cuttings description) of the wells displayed in Figure 2c were used to interpret the composition of the Zechstein Group. As a guide for the lithological interpretation of the different evaporites, we used the log values suggested by Jackson and Hudec (2017), and Warren (2018). Well 9/2-8s (Figure 2c) does not have a full set of logs for the entire Zechstein Group, and in this case the interpretation is based on the well report. The wells in this paper were selected either because they have the most complete record of the Zechstein Group (e.g., well 8/10-3 which penetrated 2 km of the Zechstein Group), or because they were drilled in strategic areas (e.g., different types of salt structures, a diapir stem, an apparent salt weld, the cap rock, a wedge-shaped geometry, or a carbonate platform). This allowed us to understand the compositional variations of the Zechstein Group in relation to the different salt structures. Wells with bottom hole temperature information (supplementary material 4) were used to create a regional geothermal gradient map for the study area. Fewer wells have been drilled in the eastern part of the study area compared to the western part, therefore the uncertainty in the geothermal gradient is higher in the eastern sector. Synthetic seismograms were constructed for the studied wells using the density and sonic logs, and the checkshots available for the sonic calibration. Well cores for the Zechstein Group were described and utilized in the study. Core material was key for the description of the cap rock. Cores of the halite unit are only available in the well 15/5-3.

The seismic dominant frequencies vary from 10 to 45 Hz, and the seismic resolution is around 35 to 40 m but can be lower. The seismic quality is good to poor. The base of the Zechstein Group is usually a continuous, high amplitude reflection, which can be easily interpreted. It is more challenging to

interpret the top of the Zechstein Group, particularly where only 2D seismic is available and amplitude contrasts are low. The flanks of the diapirs are often difficult to image (Jones and Davison 2014), therefore there is some uncertainty in this interpretation. Intra-Zechstein reflections are sometimes identified, and they can be laterally continuous throughout large regions, where deformation is minor. The identification of internal reflections depends on several factors including seismic resolution, seismic quality, deformation, among others, therefore there is uncertainty in their interpretation. The top of the Zechstein Group was converted to depth using the time-depth tables of the available wells. Most of the wells penetrating the Zechstein Group are in salt diapirs, and only few wells penetrated the salt welds. Thus, for the depth map of the Zechstein Group we have good control on the diapirs, but the uncertainty is higher in deeper areas. Seismic interpretation and time-to-depth conversion were done in DecisionSpace. The TOC data presented in this work are either in house data from the PaBas consortium (Hydrocarbon Potential of Paleozoic basins in the Central Graben, Norwegian sector-PaBas), or data available in the well reports (NPD, 2022).

4. Observations

4.1 The Zechstein Group in the NNS

In this section, the compositional variation of the Zechstein Group is described for the different salt structures present in the NNS. We have divided the salt structures into four main categories based on the amount of deformation, the height of the structures, and the thickness of the Zechstein Group. These four categories are: 1) thin beds, 2) bedded to weakly deformed evaporites, 3) intermediate size structures, and 4) tall diapirs.

4.1.1 Thin Beds: clastic and carbonate dominated Zechstein Group

Thin beds are units with low mobility and deformation, where the Zechstein Group is dominated by carbonate, clastic rocks, and anhydrite, but halite is absent (Jackson et al., 2019). The thickness of these beds is commonly 10's of m, but few wells penetrated more than 100 m. Thin beds are present in the Utsira High, Sleipner Terrace, in the NE and SE part of the Sele High, in the Fjerritslev fault complex, and between the Grensen Nose and the Feda Graben (Figures 1a, 2c). Sorento et al. (2018) and Jackson et al. (2019) have described the Zechstein Group in the Utsira High, the Sleipner Terrace, and the eastern Sele High. Thus, we will focus on the carbonate and clastic dominated Zechstein Group in the Fjerritslev fault zone, and between the Grensen Nose and the Feda Graben. Well 10/5-1 (Figure 2c) drilled an uplifted basement block in the Fjerritslev fault zone, and penetrated a 221 m thick Zechstein Group. For thin beds, the Zechstein Group is characterized by few high-amplitude continuous reflections, without major deformation (Figure 3c). In this well, the Zechstein Group can be divided into two parts: 1) A lower clastic part, which overlays the Precambrian basement, and it is characterized by tight sandstone, and calcareous claystone with fair to moderate TOC values. 2) An upper part consisting of carbonates (limestone and marls) with minor anhydrite. Locally, vuggy porosity is described, but hydrocarbons shows are not recorded (well report; NPD, 2022) (Figure 4d).

In the southwestern part of the study area (e.g., the Grensen Nose), some wells penetrated a clastic-dominated Zechstein Group (e.g., wells 2/7-31, 2/7-19, 2/7-29, 2/10-2; Figure 2c). The proportion of clastic material in these wells varies: well 2/7-31 penetrated 82 m of sandstone interbedded with claystone and minor limestone, while well 2/10-2 consists of 66 m of anhydrite interbedded with claystone and minor sandstone (Figures 3d-e) (NPD, 2022). Wells 2/9-2, 2/9-3, 2/9-4 penetrated the lower Permian Rotliegend Group, but the Zechstein Group is absent. Seismic interpretation in the SW

part of the study area is challenging due to the thin character of the Zechstein Group (less than 90 m), structural complexity, and low seismic signal at this level. Despite these challenges, a common characteristic of the wells that penetrate the clastic-dominated Zechstein Group in this area, is the proximity to a normal fault and the presence of wedge geometries within the Zechstein Group (Figures 3a-b). The wedge penetrated by well 2/10-2 is mainly of Triassic age; however, we interpret the base of the Zechstein Group at the base of the wedge. Although the Zechstein Group within this wedge consists of only two reflections, we interpret that the group pinches out to the SW, since the top Zechstein reflection becomes discontinuous and fades out laterally (Figure 3b).

4.1.2 Bedded to weakly deformed evaporites: pillows, anticlines, and low-relief rollers

Bedded to weakly deformed evaporites are thick units (approx. 1000 m) where the top of the Zechstein Group exhibits weak deformation despite the presence of halite. These units were observed in the central part of the Ling depression, the western part of the Sele High, and the southern Åsta Graben (Figure 1a). Well 17/4-1 (Figure 2c) is located in the Ling depression and penetrated the top and base of the Zechstein Group at 2665 and 3834 m respectively (a thickness of 1169 m). The base of the Zechstein Group in this well is characterized by organic-rich, radioactive claystone of the Kupferschiefer Formation followed by anhydrite interbedded with claystone (Figure 4a). Then, a 320 m halite unit (Z2 equivalent) with carbonate stringers is present. The halite is followed by a 45 m package of anhydrite interbedded with carbonate and claystone (Z3 stringers, following the nomenclature of van Gent et al., 2011). A second 445 m halite package (Z3) is interpreted overlying the Z3 stringers. This halite lacks lithological heterogeneities in its lower part, but in the upper part anhydrite stringers are observed. The upper part of the Zechstein Group is heterolithic and is composed of halite interbedded with claystone, anhydrite, and K-Mg salts (carnallite and kainite, based on the well report; NPD, 2022). The top of the Zechstein Group is characterized by 19 m of anhydrite, claystone and carbonate interpreted as the caprock.

Well 17/11-1 (Figure 2c) is located close to the boundary of the Danish Norwegian Basin and the Sele High, and drilled the top of the Zechstein Group at 2517 m, but its base was not reached. This well penetrated the upper part of the Z2 halite unit, which is characterized by the presence of K-Mg salts and claystone stringers (Figure 4b). Well 17/11-1 became stuck during drilling and was abandoned without reaching the Zechstein Group base. The presence of the K-Mg salts has been suggested as one of the possible reasons for the drilling problems (well report; NPD, 2022). Z3 stringers (composed of anhydrite-claystone) are also interpreted in the well, but they are thinner than in well 17/4-1. The Z3 halite unit has a thickness of 418 m and is characterized by the presence of anhydrite stringers. Like in well 17/4-1, the upper Zechstein Group is heterolithic, with halite interbedded with claystone, K-Mg salts, anhydrite, and carbonates. The cap rock in well 17/11-1 is characterized by 17 m of anhydrite and claystone.

The Zechstein Group in the area between the Ling depression and the Sele High varies from undeformed to gently folded (Figures 5a-d). Internally, two laterally continuous reflections can be interpreted. The lower reflection represents the Z3 stringer in well 17/4-1 (Figures 4a and 5a), but in the area around well 17/11-1 it includes the Z3 stringer, and the K-Mg salts present in the upper Z2 halite unit (Figures 4b and 5b). The Z3 stringer has high to low amplitude. In the Sele High, this reflection is slightly deformed as gentle folds, but it is undeformed to the west of well 17/4-1 in the Ling depression (Figures 5a-d). The folds in the Z3 stringer are locally disharmonic where the top of the Zechstein Group is undeformed (Figures 5a and c), or harmonic where the top of the Zechstein Group is deformed (Figure 5b). The Z3 stringer reflection was mapped in a 3D survey between wells

17/4-1 and 17-11-1 (Figure 5f). This structure map reveals a series of NE-SW folds in the northern part of the Sele High, which is bounded by normal faults of similar NE-SW strike (Figures 5e-f). In addition, to the south, NW-SE oriented folds in the Z3 stringer are also present (Figure 5f). The top of the Zechstein Group only exhibits the NW-SE folds (Figure 5g). The upper Z4 reflection represents the boundary between the Z3 halite unit and the upper heterolithic succession (Figure 5a). Along this boundary, K-Mg salts are common based on well data, and locally folds within an undeformed Zechstein Group are observed (Figure 5d). The Z3 stringer and the Z4 reflection divide the Zechstein Group into 3 seismic units. The first unit or lower part of the Zechstein Group (which mainly represents the Z2 halite unit) is characterized by low seismic amplitude and higher thickness in the hanging wall of some normal faults (Figures 5a, c, and d). The second unit is characterized by low amplitudes, where the seismic pattern varies from continuous reflections to reflection free. This second unit represents the Z3 halite and locally onlaps the Z3 stringer (Figure 5c). The third unit displays more continuous, medium amplitude reflections and coincides with the upper heterolithic part of the Zechstein Group (Figure 5a). The upper part of the Zechstein Group is commonly faulted in this area.

The Zechstein Group top in the area between the Coffee Soil fault complex and the southern Åsta Graben (Figure 1a) is also characterized by weak deformation (Figure 6d). Internally, a high amplitude, discontinuous and deformed reflection can be followed in this area (Figure 6d). The significance of this high amplitude reflection is uncertain due to the lack of well control in the area. Two wells, 3/8-1 and 3/5-1 (Figure 2c) penetrated the western boundary of this region. Well 3/8-1 penetrated a 458 m thick Zechstein Group, which has a lower heterolithic unit (anhydrite, carbonate, claystone and K-salts) followed by a 369 m thick halite-dominated unit with anhydrite stringers (Figure 6b). Well 3/5-1 penetrated a 201 m thick Zechstein Group with a lower heterolithic part composed of anhydrite, carbonate, claystone and polyhalite (described in the well report, NPD, 2022). The carbonate is described as tight but with traces of hydrocarbons (NPD, 2022). Then, two main halite units with carbonate stringers are separated by a thin unit of anhydrite, carbonate, and claystone (Z3 stringer?). The upper part of the Zechstein Group in well 3/5-1 is characterized by 21 m of anhydrite, which is interpreted as the cap rock. Well 3/5-1 was drilled close to the high amplitude reflection. If this reflection is extended to the well, it seems to coincide with the Z3 stringer (Figure 6e). An alternative interpretation is that the high amplitude reflection corresponds to the lower heterolithic part of the Zechstein Group.

4.1.3 Intermediate size salt structures

The northwestern and central parts of the study area are characterized by minibasins bounded by intermediate size salt diapirs. These diapirs usually have a height between 1000 and 2000 m, but they can be taller. Some of the diapirs are elongated and form polygonal or irregular geometries in map view, while other are isolated (Figure 2b-c) (Stewart and Clark, 1999; Karlo et al., 2014; Jackson and Hudec, 2017). Seismic interpreted salt welding (or apparent welding) is common in this area. Well 7/3-1 (Figure 2c) was drilled in an elongated salt wall (Figures 7c and 8a). In cross section, this salt wall has a narrower stem compared to the bulb, and the crest is angular (Figure 8a). In the upper part of the diapirs, continuous reflections with a similar dip than the salt crest are observed. Well 7/3-1 penetrated the base and top of the Zechstein Group at 4402 and 2696 m respectively (Figure 7c). Thin layers of organic-rich claystone interbedded with carbonate were found at the base. TOC values of 9.49% and 3.78% were measured in claystone at 4383.6 m and 4381 m, above the Kupferschiefer Formation (Skarstein personal communication, PaBas in-house data). From 4348 m to 2720 m, the well is mainly composed of halite. The proportion of anhydrite, K-Mg salts and claystone stringers is higher in the lower part. In the middle, a second zone with anhydrite layers could indicate an incipient

Z3 stringer level. The upper halite unit is relatively clean, except for two claystone stringers. The top of this well is characterized by 43 m of anhydrite and carbonate interpreted as the cap rock.

Wells 8/10-3 and 6/3-2 penetrated salt walls with dendritic map patterns (Figure 2b-c). In cross section, wider lower parts and narrower crests characterize these diapirs (Figures 8b-c). The crests tend to be flat and display high amplitudes, which we interpret as carbonate build-ups (Figure 8c). Internally, some of these diapirs have continuous parallel reflections in their upper part. Although some of these reflections can be multiples created by carbonates or the cap rock present at the top of the diapirs, we consider that some of these reflections are real, showing parallelism with the crest of the diapir. This is supported by lithological variations in well logs, which coincide with seismic reflections. The lower part of the diapirs are low amplitude and reflection free, but mounds or inclined reflections can be present (Figure 8c). Well 8/10-3 (Figure 7d) penetrated the base and top of the Zechstein Group at 5398 and 3394 m respectively. This well has a heterolithic lower part characterized by thin layers of carbonate and claystone, followed by halite, interbedded with claystone and anhydrite stringers. The claystone stringers in this well are thicker in comparison to other wells in the area. The lower heterolithic composition correlates with the mounds and inclined seismic reflections. The upper part of the well is halite dominated but the serrate pattern of the DT log suggests high amount of anhydrite stringers. The top of well 8/10-3 is characterized by 59 m of anhydrite, claystone and carbonate interpreted as the cap rock. Well 6/3-2 crosses the Zechstein Group in a hanging wall block (Figure 8b). This well penetrated the base and top of the Zechstein Group at 4045 and 3293 m respectively (Figure 7b). The lower part of the Zechstein Group in the well is characterized by claystone interbedded with carbonate, with moderate organic matter content (TOC values of 1.34% and 0.42% at depths of 4030 m and 4040 m; NPD, 2022). Moving upwards, a first halite unit (Z2) of 192 m is present containing claystone and anhydrite stringers, followed by a layer of anhydrite and claystone which is interpreted as the Z3 stringer. A second 370 m halite unit (Z3) with claystone stringers overlies the Z3 stringer. The upper 100 m of this well is characterized by anhydrite, carbonate and claystone interpreted as the cap rock. K-Mg salts are absent in both wells 8/10-3 and 6/3-2.

Well 16/7-1 (Figure 2c) penetrated the upper part of a triangular diapir (Figure 8d). The top of the Zechstein Group was reached at 2085 m (Figure 7a). This well drilled a main halite unit with high amount of anhydrite and claystone stringers. The presence of deformed evaporitic beds apparently caused excessive well deviation and other drilling problems and the well was abandoned without reaching its final objective (well report, NPD, 2022). The cap rock in this well is interpreted to be 45 m and is composed of anhydrite, carbonate, and claystone.

In the Søgne Basin, well 3/7-2 (Figure 2c) drilled a salt diapir with high amplitude reflections in its upper part (Figure 6f). The top and base of the Zechstein Group were reached at 2998 and 4166 m, respectively (Figure 6a). Well 3/7-2 penetrated a lower part composed of anhydrite, carbonate and claystone followed by a main halite unit interbedded with thick K-salts. The upermost K-salt layer has a thickness of 150 m. The well report describes the K-salts as sylvinite (halite and sylvite). Dipmeter measurements in the K-salts indicate dip angles of 60 to 70°, suggesting internal deformation (NPD, 2022). The high amplitude reflections at the top of the diapir coincide with the upper 150 m thick K-salt unit.

4.1.4 Tall diapirs

Shallow salt stocks and walls are present in the eastern and southwestern parts of the study area (e.g., the Egersund basin, Figure 1a). Some of these structures can have lengths of 60 km and heights of 4 km (Figures 2b and 9). There are no wells that fully penetrate these salt structures; however, four key wells contribute to the understanding of compositional variations. Well 8/3-1 (Figure 2c) was drilled

in the flank of one asymmetric diapir in the faulted boundary between the Egersund Basin and the Sele High. Internally, the diapir flank is divided into two main seismic packages, a lower unit with low amplitude and reflection free and an upper unit with parallel, continuous, medium to high amplitude reflections (Figure 9c). Well 8/3-1 penetrated the top and the base of the Zechstein Group at 2205m and 2965 respectively (Figure 10a). The lower part of the Zechstein Group is characterized by a thin unit of claystone and carbonate followed by a main halite unit of 673 m with K-Mg salts stringers. In the upper part of the Zechstein Group, an 80 m anhydrite interbedded with carbonate and claystone is interpreted as the cap rock. K-Mg salt layers are more common in the upper part of the halite sequence in this well, and together with the cap rock they correspond with the high amplitude, continuous reflections on the seismic section (Figure 9c). Well 9/2-8s (Figure 2c) was drilled through a narrow diapir stem with a wider bulb within the Egersund Basin (Figure 9b; Jackson and Lewis, 2012). This well penetrated an anhydrite bed at the diapir margin, followed by a halite unit with multiple K-Mg salts and minor anhydrite inclusions (Figure 10b) (well report, NPD, 2022). An anhydrite layer followed by a clastic claystone-sandstone succession characterizes the other (SW) diapir boundary. Well 1/6-5 (Figure 2c) was drilled through the crest of a similar salt diapir with narrow stem and wider bulb (Figure 9a). This well penetrated the Zechstein Group top at 1742 m and found 106 m of anhydrite interbedded with thin layers of claystone, interpreted as the cap rock, followed by halite at the base of the well (Figure 10c). In the Egersund basin, well 9/4-5 drilled through a seismic interpreted weld (Figures 2c and 9d). This well penetrated a 55 m Zechstein Group, which is claystone dominated at the bottom and carbonate dominated at the top (Figure 4c). The carbonate is interbedded with halite and TOC values of 3.32% were measured between 5215 and 5243 m (NPD, 2022).

4.2 Cap rock and halite heterogeneities

The cap rock has high variability in composition, thickness, and deformation. The cap rock is thinner in bedded salt to weakly deformed evaporites, and it is thicker in tall diapirs. In well 3/8-1 the cap rock was absent, whereas in well 1/6-5 it has a thickness of 106 m (Table 1). The composition of the cap rock varies from anhydrite-dominated with claystone or siltstone stringers, and where carbonate is absent (e.g., well 1/6-5), to wells where carbonate (e.g., dolomite) is present together with anhydrite, clastic rocks or celestite (Figure 11 c-h). Different deformation structures are identified in the cap rock including veins, folds, boudins of high competent lithologies embedded in anhydrite, and breccias (Figures 11c, d, g, and h). Fractures are commonly associated with the presence of siltstone stringers, but they are also observed within anhydrite (Figure 11f). Shows of hydrocarbons were reported in the cap rock in well 2/8-13 (Figure 2c; NPD, 2022).

Only well 15/5-3 (Figure 2c) has cores available for the halite unit. The halite varies from containing low number of stringers (Figure 11b) to halite with discontinuous stringers of anhydrite and claystone (Figure 11a, right core). Halite with K-salts was also observed (Figure 11a, left core). The core with K-salts is notoriously thinner and more fragile.

4.3 Depth of the Zechstein Group and geothermal gradient

Since most salt caverns for subsurface storage are located between 500 to 2000 m (Warren, 2006; Gillhaus and Horvath, 2008), it is important to describe the variation in depth of the salt structures in the study area (Figure 12a). Figure 12b shows the areas in the NNS where the Zechstein Group is shallower that 2000 m. The salt structures that fulfill this depth criterion are tall diapirs and some intermediate size salt structures in areas such as the Egersund Basin, Åsta Graben, Danish Norwegian

basin, and the Sørvestlandet High. Salt creep rate increases with temperature (Le Comte, 1965; Warren, 2006; Jackson and Hudec, 2017). Thus, basin temperatures should be considered before selecting a location for salt cavern construction. In the NNS, the geothermal gradient varies considerably. High geothermal gradients (40-50 °C/km) are observed in the Central Graben and low geothermal gradients (20-30 °C/km) are observed in the eastern side (Figure 12c). Thus, on the tall diapir penetrated by well 1/6-5 to the SW (Figure 9a), the bottom hole temperature is 104℃ at 1854 m, while in well 17/11-1 drilled in a weakly deformed zone to the NE (Figure 5b), the temperature is 83℃ at 3269 m (Figure 12c; NPD, 2022). The maximum temperature for a safe salt cavern with low creep is considered to be ~80℃ (Gregorowicz et al. 1996; Merey, 2019). Therefore, it is the deeper NE well the one that is still within the maximum temperature boundary. This well has also higher confining (overburden) pressure, which should decrease the salt creep rate (Le Comte, 1965), but low viscosity K-Mg salts which can facilitate creep (Figure 4b).

5. Discussion

5.1 Compositional variation of the Zechstein Group on different salt structures

To describe the compositional variation of the Zechstein Group in the NNS (Figure 2a), we have modified the depositional zones from Clark et al. (1998) and other works such as van Adrichem Boogaert and Kouwe, 1993; Taylor (1998); Sorento et al. (2018); Jackson et al. (2019); Pichat (2022), and the wells from this study (Figure 2c). As in other North European regions, the Zechstein Group in the NNS is characterized by a shallow part dominated by carbonate, clastic rocks, and anhydrite, where halite is absent. These carbonate-dominated platforms are in parts of the Utsira High, the Sleipner Terrace, the NE and SE parts of the Sele High, the uplifted footwalls along the Fjerritslev fault complex, and between the Grensen Nose and the Feda Graben (Figures 1a and 12d). The observed wedge-shaped geometries in the clastic-dominated Zechstein Group (Figures 3a and b), and the absence of this group in some wells in the SW part of the study area (Figure 12d), suggest Permo-Triassic intra-Zechstein syn-kinematic strata, bounded by active normal faults. The lack of halite and K-Mg salts in these wells indicates shallow water depth (Taylor, 1998).

At intermediate water depths, halite units contain stringers of different composition: carbonate, claystone, and anhydrite, changing into anhydrite, claystone, and K-Mg salts in deeper waters (Figures 2a and 12d). This composition is mainly observed in the western part of the study area, and it is linked to intermediate size salt structures. With the available data it is difficult to separate areas with or without K-Mg salts. However, the few wells without K-Mg salts are located where the thickness and the height of the salt structures are low (wells 6/3-2, 8/10-3, and 3/5-1; Figure 2b-c). Wells containing different stringers including K-Mg salts penetrate taller diapirs, usually with triangular shape or with a stem narrower than the bulb (wells 7/3-1 and 16/7-1; Figure 8a, d).

The deepest part of the basin is dominated by halite with K-Mg salts stringers and only minor anhydrite and claystone (Figures 2a and 12d). Wells 8/3-1 and 9/2-8S exhibit this composition and penetrate the tallest diapirs with heights up to 4 km in the Egersund basin (Figures 9b-c and 10a-b). The well 3/7-2 has also this composition, but it is in the south of an intermediate size salt structure (Figure 6a, f).

Based on the well and seismic data, there seems to be a correlation between the tallest diapirs and the presence of K-Mg salts. This is probably explained because K-Mg salts with thick halite were preferentially deposited in the deepest part of the basin. Since more ductile and lower viscosity evaporites were available, the salt diapirs could grow higher. Rowan et al. (2019) discuss that stringers of competent lithologies can have high angles within salt diapirs and therefore there is a lower

probability to be penetrated by wells. Compositional fractionation has also been described during salt flow (Kupfer, 1968). These two conditions highlight the potential interpretation bias of using wells to interpret the composition of salt diapirs. However, well 8/3-1 (Figures 9c and 10a) penetrated a moderately deformed Zechstein Group dominated by halite and K-Mg salts on the flank of a tall salt diapir. The mild deformation of the Zechstein Group in this area, reduces the change of high-angle stringers of competent lithologies, and compositional fractionation. Thus, this well supports that the central part of the study area was deep and halite dominated with the presence of K-Mg stringers (Figure 12d). Clearly, composition is not the only factor controlling the size of the diapirs. Weakly deformed or bedded salt in the Ling depression and the western part of the Sele High are also halite dominated with a mix of stringers, including K-Mg salts. Additionally, the salt diapir penetrated by well 3/7-2 is K-salt and halite dominated (Figure 6a, f). However, this structure is smaller than the diapirs in the Egersund Basin. Therefore, it is the triggering mechanism of salt deformation, the thickness of the halite plus K-Mg salts, sedimentation rate vs. salt rise rate, among others which conditioned the presence of tall diapirs in the region. Previous studies have divided the Zechstein Group into non-mobile and mobile parts (e.g., Clark et al., 1999; Duffy et al., 2013; Jackson et al., 2019). This study emphasizes the complexity of the mobile part of the Zechstein Group, where salt structures vary from weakly deformed salt to tall isolated diapirs with several internal heterogeneities.

5.2 Internal deformation of the Zechstein Group

Layer conformity: Parallel conformable reflections are commonly observed in the upper part of the different salt structures. Reflections are mainly absent in the inner parts of the diapirs (Figures 8a, b, d, and 9c). This pattern is the result of 1) *lithological variations*: In areas where the Zechstein Group has weak deformation, the parallel conformable reflections indicate a heterogeneous composition in the upper Zechstein Group (see wells 17/4-1, 17/11-1, and 8/3-1). On the other hand, the low-amplitude, reflection free package indicates halite-rich units (Figures 5a-b, and 9c). Seismic lines in the Dutch North Sea shows a similar pattern (Van Gent et al., 2011; Raith et al., 2015). 2) *Deformation*: The well 16/7-1 penetrates a compositionally heterogeneous triangular diapir (Figure 8d). Parallel reflections in this salt structure are observed in the upper part of the diapir, but they are not present inwards, indicating complex deformation in the inner part of the diapir (Jackson and Hudec, 2017). 3) *Multiples*: the diapir penetrated by well 7/3-1 displays reflections in its upper part parallel to the crest, but in a package of homogeneous halite (Figures 7c and 8a). We suggest that in this case the more likely explanation is the presence of multiples. The internal reflection in the upper part of the tall diapir from the Egersund Basin (Figure 9b) is an interesting case. This reflection has no well control, and we speculate it can either be an intralayer (e.g., K-Mg salt or even anhydrite), the contact between the cap rock and the halite, or a multiple (although there is a lack of multiple reflection repetitions). Summarizing, in the weakly deformed and some of the intermediate size salt structures, the seismic character can help to recognize the upper heterolithic part of the Zechstein Group and the boundary between the halite rich Z2 and Z3 units (characterized by stringers, and the presence of K-Mg salts).

Disharmonic folds: Two types of disharmonic folds have been observed in the study area: 1) folding of the Z2 halite unit and the Z3 stringer, where the upper Zechstein Group is undeformed and onlaps the Z3 stringer, indicating syn-depositional deformation (Figures 5a and c). One of the potential triggers for this deformation is an extensional event. This is supported by the similar orientation of the intra Zechstein folds and the faults in the northern part of the Sele High, and the presence of thicker evaporites in the hanging walls of these faults (Fig. 5e-f). 2) Disharmonic folds embedded in an undeformed Zechstein Group in the Ling depression (Figure 5d). These folds were observed at the boundary between the Z3 halite unit and the upper heterolithic succession Z4, where K-Mg salts are

common (Z4 reflection in Figure 5d). We suggest that the disharmonic folds were triggered by slope instability associated to topographic variations (gravity gliding). This is reasonable since the Ling depression was surrounded by shallow carbonate platforms (Figure 12d).

Thickening of K-Mg salts: The well 3/7-2 penetrated 150 m thick K-salts with high dipmeter angles at the crest of a salt diapir (Figure 6a, f). We suggest that this high thickness is the result of the flow of the K-salts into the upper part of the salt diapir. Thickening of K-Mg salts have been described in the Zechstein Group in other countries, either at the crest or in the flanks of the diapirs (Coelewij et al.; 1978; Szymaniak, et al., 2002; Raith et al., 2015).

Highly disturbed and disrupted stringers: boudins of competent siltstone are observed within anhydrite in the caprock, and within halite in cores (Figure 11a, d). Highly disturbed and disrupted stringers are observed in the SW part of the study area on seismic lines (Figure 6d). Similar boudins and stringers disruption have been described by Van Gent et al. (2011), Rowan et al. (2019), and Jackson and Hudec (2017). They are explained as the result of extension of competent layers embedded into a weak matrix. Other structures such as faults and veins have been observed at diapir crests. Characterizing the internal deformation of salt structures is relevant because they can be associated to preferential shear zones, which are important to understand both in terms of geometry and kinematics to minimize risk (Duffy et al., 2022).

5.3 Implications for source rocks and reservoirs

The Kupferschiefer Formation is usually not considered a source rock in the North Sea due to its limited thickness and because it is sealed by evaporites (Jackson and Stewart, 2017). Geochemical studies in the Kupferschiefer Formation in the NNS suggest that this formation has potential for oil generation (Pedersen et al., 2006). In this study, we have described different organic-rich intervals in the Zechstein Group. The first Zechstein cycle has two widespread organic-rich levels, the Kupferschiefer Formation and a second claystone where TOC values of 9.48% have been measured (Skarstein personal communication, PaBas in-house data) (Figure 7c). Additionally, other intra Zechstein Group layers have moderate to high TOC values in claystone or carbonate (Figure 4c-d). These observations indicate that the upper Permian source rock potential is not restricted to the Kupferschiefer Formation. Additionally, these organic rich rocks are not always encased in thick evaporites, seismic welding areas can contain organic-rich rocks and could have acted as migration windows (Figures 4c and 9d).

The Zechstein carbonates are a common reservoir target in different countries (Taylor 1998). Carbonates of the Zechstein Group in the study area were formed in three different ways: 1) carbonates deposited in shallow marine conditions (Figure 2a). For the NNS, Sorento et al. (2018) and the available well reports indicate that these carbonates can have good to bad reservoir properties. 2) Cap rock carbonates: In areas such as the Gulf of Mexico the cap rock limestones are proven reservoirs where porosity is enhanced due to dissolution, fracturing, and chemical alteration (Posey and Kyle, 1998; Jackson and Hudec, 2017). The potential of the cap rock as reservoir in the NNS is uncertain. In few wells, carbonates and celestite with hydrocarbons shows are interpreted (Figure 11e). However, in other wells the cap rock is dominated by anhydrite and carbonates are absent. Other factor that is difficult to predict is the thickness of the cap rock, whereas in some wells the cap rock is absent (e.g., well 3/8-1), in other wells it can reach a thickness of more than 100 m (wells 6/3-2 and 1/6-5, Table 1 and Figure 2c). Thus, the cap rock tends to be thicker in intermediate size to tall diapirs and thinner or absent in the weakly deformed areas. 3) Finally, carbonate buildups can be formed when diapirs produce seafloor highs (Giles et al., 2018; Roca et al., 2021). Mound seismic facies have been interpreted on a diapir roof in the western part of the study area, coinciding with carbonates in

the well logs (Figures 7d and 8c), which suggest that some diapirs were exposed or close to the sea floor.

5.4 Challenges and opportunities for subsurface storage

In different salt cavern studies, salt deposits are classified either as bedded salt or as salt domes (e.g., Yang et al., 2013; Tarkowski and Czapowski, 2018; Tarkowski, 2019; Caglayan et al. 2020). As noted by Gillhaus and Horvath (2008), salt caverns have been built in a great diversity of salt structures, and for a better selection of salt cavern location, these differences must be characterized. Except for the thin beds where halite is absent, in all the other salt structures described in this study, weakly deformed structures, intermediate size salt structures, and tall diapirs, halite beds of more than 300 m are present. Therefore, the thickness criterium for salt cavern construction is fulfilled in the NNS. The weakly deformed structures present high predictability (although internal folding is present), partially because the seismic image is better and internal reflections can be followed (Figure 5a). The two main halite units (Z2 and Z3) in these structures are expected to have lateral continuity (e.g., the Z3 halite has a thickness of 445 m in well 17/4-1 and 418 m in well 17/11-1; Figures 4a-b). Other advantages of the weakly deformed structures are that the cap rock is thin or absent (Table 2), and for the Ling depression and the Sele High, the geothermal gradients are usually lower than 30°C/km. However, the weakly deformed structures are deeper than 2000 m, and high overburden pressures are expected.

For the intermediate size structures, the polygonal map pattern can provide large storage areas. However, some of these structures are deeper than 2000 m and they are close to the Central Graben where the geothermal gradient can be higher than 40°C/km. Thus, high temperatures are expected within the salt, which will increase the risk of creep. Tall diapirs are usually shallower than 2000 m and some are elongated structures (salt walls), which can provide large areas for storage. Additionally, their shallow depth can make them more attractive due to economic considerations and the current technology. However, tall diapirs have not been fully penetrated by wells, and there is poor lithological control. In addition, these structures exhibit high deformation and poor seismic image, and therefore it is challenging to predict their compositional variability from seismic and well interpretation.

The cap rock can be particularly thick (about 100 m) in intermediate size and tall salt structures. The presence of breccias, veins, fractures and faults, and lithological variations indicate that the cap rocks are poor seals and can be migration pathways if the roof of a cavern intercepts them. In all the structures, different stringers are present. K-Mg stringers apparently dominate in tall diapirs and in some intermediate size structures. In these cases, thickening of K-Mg salts can occur at the diapir crest or in the flanks (Figure 6a) (Coelewij et al.; 1978; Szymaniak, et al., 2002; Raith et al., 2015). A mix of competent stringers (anhydrite, claystone, and carbonate) with weak K-Mg salts is observed in weakly deformed evaporites and intermediate size salt structures (Figures 4a-b). As described in other parts of Europe, K-Mg salts are usually present in the upper part of the Z2 and Z3 halite units (Pichat, 2022). This observation is useful for the prediction of K-Mg salts in weakly deformed evaporites, but in diapiric structures, higher internal deformation makes this prediction more challenging. However, K-Mg salts are not always present in the upper part of the Z2 halite unit. For instance, well 17/4-1 lacks K-Mg salts at the top of the Z2 halite and exhibits a thick Z3 stringer (Figure 4a), suggesting shallower waters than in well 17/11-1 where the K-Mg salts are present in the upper part of the Z2 halite unit (Figure 4b). The stringers within the halite can contribute to cavern irregularities, fluid contamination and migration pathways (Warren, 2006; Kruck et al., 2013; Panfilov, 2016; Hemme and van Berk, 2017; Jackson and Hudec, 2017, Looff, 2017; Cyran, 2020; Portarapillo and Di Benedetto, 2021). In case of penetration of thick K-Mg salts, as in well 3/7-2 (Figure 6a), creep can be significantly enhanced (Warren, 2006). However, the proportion of stringers matters, and when they are a small percentage,

the bulk rocks properties are not affected as much (Jackson and Hudec, 2017). We have described the geological feasibility for underground storage offshore Norway in the North Sea. Offshore storage projects and technology are being developed in the UK North Sea (e.g., the Gateway storage facility and Tractebel technological development). We have not discussed cost considerations, but the economic feasibility of NNS salt storage projects will depend on different factors such as large-scale use of hydrogen, the demand for subsurface energy storage, and technological developments including the repurposing of current infrastructure (Allsop et al., 2023).

Conclusions

- Salt structures in the NNS area are divided into four categories: 1) thin beds, which are either carbonate or clastic dominated, and where halite is absent. 2) Bedded salt to weakly deformed evaporites; 3) intermediate size salt structures; and 4) tall diapirs, including salt stocks and walls. The last three categories are halite-dominated.
- Halite beds of more than 300 m thickness have been recognized in the main salt structures, suggesting an opportunity for underground storage in salt caverns. One of the challenges associated to bedded salt and intermediate salt structures is the depth of the halite units, which is usually more than 2000 m. A second challenge is the presence of thin layers of both more and less competent lithologies within the halite, which can lead to cavern size anomalies due to different dissolution properties. The presence of K-Mg salts and high temperatures can enhance the risk of creep. In tall diapirs, it is difficult to predict internal composition due to high deformation and poor seismic image. Additionally, these diapirs can contain K-Mg salt.
- The thickness, composition and deformation structures in the cap rock vary significantly, potentially affecting its sealing properties. The cap rock is thicker in tall diapirs, and it includes competent and, in some cases, porous rocks such as celestite, anhydrite, dolomite, siltstones and shales. Breccias, veins and faults can be present in cap rocks.
- Tectonics and syn-sedimentation are interpreted during the late Permian. First, normal faulting created uplifted footwalls and clastic dominated Zechstein growth strata to the SW of the NNS. Second, intra Zechstein salt tectonics created disharmonic folds within the Z2 halite unit and the Z3 stringer.
- Different organic rich intervals are present in the Zechstein Group in addition to the Kupferschiefer Formation. Seismic welds can also contain organic rich rocks and act as hydrocarbon migration pathways. Carbonates are interpreted in the cap rock and as carbonate build ups at the top of the diapirs, in addition to the well-known Zechstein Group shallow water carbonates.

References

ALLSOP, C., YFANTIS, G., PASSARIS, E., & EDLMANN, K. (2023). Utilising publicly available datasets for identifying offshore salt strata and developing salt caverns for hydrogen storage. *Geological Society, London*, Special Publications, **528(1**), SP528-2022.

CAESAR, K., KYLE, J., LYONS, T., TRIPATI, A. & LOYD, S. (2019) Carbonate Formation in Salt Dome Cap Rocks by Microbial Anaerobic Oxidation of Methane. *Nature communications*, **10,** 1-9.

CAGLAYAN, D.G., WEBER, N., HEINRICHS, H.U., LINßEN, J., ROBINIUS, M., KUKLA, P.A. & STOLTEN, D. (2020) Technical Potential of Salt Caverns for Hydrogen Storage in Europe. *International Journal of Hydrogen Energy*, **45,** 6793-6805.

CLARK, J., CARTWRIGHT, J. & STEWART, S. (1999) Mesozoic Dissolution Tectonics on the West Central Shelf, Uk Central North Sea. *Marine and Petroleum Geology*, **16,** 283-300.

CLARK, J., STEWART, S. & CARTWRIGHT, J. (1998) Evolution of the Nw Margin of the North Permian Basin, Uk North Sea. *Journal of the Geological Society*, **155,** 663-676.

COELEWIJ, P. & KUIJK, V. (1978) Magnesium-Salt Exploration in the Northeastern Netherlands. *Netherlands Journal of Geosciences/Geologie en Mijnbouw,* **57**, (4), 487-502.

CROTOGINO, F. (2016) Traditional Bulk Energy Storage—Coal and Underground Natural Gas and Oil Storage. In: *Storing Energy* (Ed. By Letcher T.M.) 633-649. Elsevier.

CYRAN, K. (2020) Insight into a Shape of Salt Storage Caverns. *Archives of Mining Sciences*, **65,** 363-398.

DAVISON, I., ALSOP, G., EVANS, N. & SAFARICZ, M. (2000) Overburden Deformation Patterns and Mechanisms of Salt Diapir Penetration in the Central Graben, North Sea. *Marine and Petroleum Geology*, **17,** 601-618.

DUFFY, O.B., GAWTHORPE, R.L., DOCHERTY, M. & BROCKLEHURST, S.H. (2013) Mobile Evaporite Controls on the Structural Style and Evolution of Rift Basins: Danish Central Graben, North Sea. *Basin Research*, **25,** 310-330.

DUFFY, O.B., MOSCARDELLI, L., HUDEC, M.R., DOOLEY, T.P., PEEL, F., LOOFF, K., APPS, G. & SHUSTER, M.W. (2022). *Potential Controls on the Origin, Nature and Distribution of Shear Zones in Salt Stocks: Salt Tectonic Insights with a Solution Mining Perspective*. Solution Mining Research Institute, Technical Conference. 26 p.

ELLIOTT, G.M., JACKSON, C.A.L., GAWTHORPE, R.L., WILSON, P., SHARP, I.R. & MICHELSEN, L. (2021) Tectono-Stratigraphic Development of a Salt-Influenced Rift Margin: Halten Terrace, Offshore Mid-Norway. *Basin Research*, **33,** 3295-3320.

GILES, K.A., ROWAN, M.G., LANGFORD, R. & HEARON, T. (2018) Salt Shoulders. *AAPG search and discovery article*, **30554**.

GILLHAUS, A. & HORVATH, P. (2008) Compilation of Geological and Geotechnical Data of Worldwide Domal Salt Deposits and Domal Salt Cavern Fields. *Solution Mining Research Insitute and KBB Underground Technologies GmbH, Clarks Summit, PA, USA*. 201 p

GLENNIE, K., HIGHAM, J., STEMMERIK, L., EVANS, D., GRAHAM, C., ARMOUR, A. & BATHURST, P. (2003) Permian. *The Millennium Atlas: Petroleum Geology of the Central and Northern North Sea. Geological Society, London*, **91,** 103.

GLENNIE, K. & UNDERHILL, J. (1998) Origin, Development and Evolution of Structural Styles. *Petroleum geology of the North Sea: Basic concepts and recent advances*, 42-84.

Gregorowicz, J., Peters, C., de Swaan Arons, J., Friedrichs, G. & Jaeschke, M. (1996) Phenomena Related to the Storage of Natural Gas in Underground Caverns. *Fluid Phase Equilibria*, **117,** 249-256.

Hemme, C. & van Berk, W. (2017) Potential Risk of H2s Generation and Release in Salt Cavern Gas Storage. *Journal of Natural Gas Science and Engineering*, **47,** 114-123.

Jackson, C.A.L., Elliott, G.M., Royce-Rogers, E., Gawthorpe, R.L. & Aas, T.E. (2019) Salt Thickness and Composition Influence Rift Structural Style, Northern North Sea, Offshore Norway. *Basin Research*, **31,** 514-538.

Jackson, M.P. & Hudec, M.R. (2017) *Salt Tectonics: Principles and Practice.* Cambridge University Press. 498 p

Jackson, C.A.-L. & Lewis, M.M. (2012) Origin of an Anhydrite Sheath Encircling a Salt Diapir and Implications for the Seismic Imaging of Steep-Sided Salt Structures, Egersund Basin, Northern North Sea. *Journal of the Geological Society*, **169,** 593-599.

Jackson, C.A.L. & Lewis, M.M. (2016) Structural Style and Evolution of a Salt-Influenced Rift Basin Margin; the Impact of Variations in Salt Composition and the Role of Polyphase Extension. *Basin Research*, **28,** 81-102.

Jackson, C.-L. & Stewart, S. (2017) Composition, Tectonics, and Hydrocarbon Significance of Zechstein Supergroup Salt on the United Kingdom and Norwegian Continental Shelves: A Review. *Permo-Triassic Salt Provinces of Europe, North Africa and the Atlantic Margins*, 175-201.

Jones, I. F., & Davison, I. (2014). Seismic imaging in and around salt bodies. *Interpretation*, **2**, SL1-SL20.

Kairanov, B., Escalona, A., Norton, I. & Abrahamson, P. (2021) Early Cretaceous Evolution of the Tromsø Basin, Sw Barents Sea, Norway. *Marine and Petroleum Geology*, **123,** 104714.

Kalani, M., Faleide, J.I. & Gabrielsen, R.H. (2020) Paleozoic-Mesozoic Tectono-Sedimentary Evolution and Magmatism of the Egersund Basin Area, Norwegian Central North Sea. *Marine and Petroleum Geology*, **122,** 104642.

Kane, K.E., Jackson, C.A.-L. & Larsen, E. (2010) Normal Fault Growth and Fault-Related Folding in a Salt-Influenced Rift Basin: South Viking Graben, Offshore Norway. *Journal of Structural Geology*, **32,** 490-506.

Karlo, J.F., van Buchem, F.S., Moen, J. & Milroy, K. (2014) Triassic-Age Salt Tectonics of the Central North Sea. *Interpretation*, **2,** SM19-SM28.

Koyi, H.A. (2001) Modeling the Influence of Sinking Anhydrite Blocks on Salt Diapirs Targeted for Hazardous Waste Disposal. *Geology*, **29,** 387-390.

Kruck, O., Crotogino, F., Prelicz, R. & Rudolph, T. (2013) Assessment of the Potential, the Actors and Relevant Business Cases for Large Scale and Seasonal Storage of Renewable Electricity by Hydrogen Underground Storage in Europe. *KBB Undergr. Technol. GmbH*. 94 p.

Kupfer, D. H. (1968). Relationship of internal to external structure of salt domes. *AAPG Mem.*, **8**, 79-89

Kumar, K., Makhmutov, A., Spiers, C.J. & Hajibeygi, H. (2021) Geomechanical Simulation of Energy Storage in Salt Formations. *Scientific Reports*, **11,** 1-24.

Le Comte, P. (1965) Creep in Rock Salt. *The Journal of Geology*, **73,** 469-484.

Lewis, M.M., Jackson, C.A.-L. & Gawthorpe, R.L. (2013) Salt-Influenced Normal Fault Growth and Forced Folding: The Stavanger Fault System, North Sea. *Journal of Structural Geology*, **54,** 156-173.

Looff, K., Duffield, J. & Looff, K. (2003). *Edge of Salt Definition for Salt Domes and Other Deformed Salt Structures–Geologic and Geophysical Considerations*. SMRI Spring Technical Conference, Citeseer. 20 p.

Looff, K. (2017). *The Impact of Anomalous Salt and Boundary Shear Zones on Salt Cavern Geometry, Cavern Operations, and Cavern Integrity*. Proc. SMRI Spring Meeting, Albuquerque, New Mexico. 31 p.

Merey, S. (2019) Prediction of Pressure and Temperature Changes in the Salt Caverns of Tuz Golu Underground Natural Gas Storage Site While Withdrawing or Injecting Natural Gas by Numerical Simulations. *Arabian Journal of Geosciences*, **12,** 1-21.

NPD (2022) Norwegian Petroleum Directorate Factpages. Retrieved from http://factp ages.npd.no/factp ages/Defau lt.aspx?cultu re=en

Ozarslan, A. (2012) Large-Scale Hydrogen Energy Storage in Salt Caverns. *International journal of hydrogen energy*, **37,** 14265-14277.

Panfilov, M. (2016) Underground and Pipeline Hydrogen Storage. In: *Compendium of Hydrogen Energy* (Ed. by, Gupta R.B., Basile, A., and Veziroglu T.N.) 91-115. Elsevier.

Parkes, D., Evans, D., Williamson, P. & Williams, J. (2018) Estimating Available Salt Volume for Potential Caes Development: A Case Study Using the Northwich Halite of the Cheshire Basin. *Journal of Energy Storage*, **18,** 50-61.

Pedersen, J.H., Karlsen, D.A., Lie, J.E., Brunstad, H. & di Primio, R. (2006) Maturity and Source-Rock Potential of Palaeozoic Sediments in the Nw European Northern Permian Basin. *Petroleum Geoscience*, **12,** 13-28.

Pichat, A. (2022) Stratigraphy, Paleogeography and Depositional Setting of the K–Mg Salts in the Zechstein Group of Netherlands—Implications for the Development of Salt Caverns. *Minerals*, **12,** 486.

Portarapillo, M. & Di Benedetto, A. (2021) Risk Assessment of the Large-Scale Hydrogen Storage in Salt Caverns. *Energies*, **14,** 2856.

Posey, H.H. & Kyle, J.R. (1988) Fluid-Rock Interactions in the Salt Dome Environment: An Introduction and Review. *Chemical Geology*, **74,** 1-24.

RAITH, A., URAI, J., STROZYK, F. & VISSER, J. (2015) Evolution of Rheologically Heterogeneous Salt Structures: A Case Study from the Northeast of the Netherlands. *Solid Earth Discussions*, **7**. 1877-1908.

REITENBACH, V., GANZER, L., ALBRECHT, D. & HAGEMANN, B. (2015) Influence of Added Hydrogen on Underground Gas Storage: A Review of Key Issues. *Environmental Earth Sciences*, **73,** 6927-6937.

ROCA, E., FERRER, O., ROWAN, M.G., MUÑOZ, J.A., BUTILLÉ, M., GILES, K.A., ARBUÉS, P. & DE MATTEIS, M. (2021) Salt Tectonics and Controls on Halokinetic-Sequence Development of an Exposed Deepwater Diapir: The Bakio Diapir, Basque-Cantabrian Basin, Pyrenees. *Marine and Petroleum Geology*, **123,** 104770.

ROJO, L.A. & ESCALONA, A. (2018) Controls on Minibasin Infill in the Nordkapp Basin: Evidence of Complex Triassic Synsedimentary Deposition Influenced by Salt Tectonics. *Aapg Bulletin*, **102,** 1239-1272.

ROJO, L.A., MARÍN, D., CARDOZO, N., ESCALONA, A. & KOYI, H. (2020) The Influence of Halokinesis on Prograding Clinoforms: Insights from the Tiddlybanken Basin, Norwegian Barents Sea. *Basin Research*, **32,** 979-1004.

ROWAN, M.G., URAI, J.L., FIDUK, J.C. & KUKLA, P.A. (2019) Deformation of Intrasalt Competent Layers in Different Modes of Salt Tectonics. *Solid Earth*, **10,** 987-1013.

SMITH, R., HODGSON, N. & FULTON, M. (1993). *Salt Control on Triassic Reservoir Distribution, Ukcs Central North Sea*. Geological Society, London, Petroleum Geology Conference series. Ed. By J. R. Parker. 547– 557

SORENTO, T., STEMMERIK, L. & OLAUSSEN, S. (2018) Upper Permian Carbonates at the Northern Edge of the Zechstein Basin, Utsira High, Norwegian North Sea. *Marine and Petroleum Geology*, **89,** 635-652.

STEWART, S. (2007) Salt Tectonics in the North Sea Basin: A Structural Style Template for Seismic Interpreters. Special Publication-Geological Society of London, 272, 361–396.

STEWART, S. & CLARK, J. (1999). *Impact of Salt on the Structure of the Central North Sea Hydrocarbon Fairways*. Geological Society, London, Petroleum Geology Conference series (Ed. By Fleet A.J., Boldy S.A.R.) 179-200.

STROZYK, F. (2017) The Internal Structure of the Zechstein Salt and Related Drilling Risks in the Northern Netherlands. In: *Permo-Triassic Salt Provinces of Europe, North Africa and the Atlantic Margins* (Ed. By Soto, J.I., Flinch, J.F., Tari, G.), 115-128. Elsevier.

SZYMANIAK, T. & SCHÄFER, M. (2002) Geologisch-Tektonische Kartierung Der Salzstruktur Asse Im Subhercynen Becken. *Technische Universität Clausthal, Institut für Geologie und Paläontologie: Clausthal-Zellerfeld, Germany*.

SØRENSEN, S., MORIZOT, H. & SKOTTHEIM, S. (1992) A Tectonostratigraphic Analysis of the Southeast Norwegian North Sea Basin. In: *Structural and Tectonic Modelling and Its*

Application to Petroleum Geology (Ed. by, R. M. Larsen, H. Brekke, B. T. Larsen, & E. Talleraas) 19-42. Elsevier.

TARKOWSKI, R. (2019) Underground Hydrogen Storage: Characteristics and Prospects. *Renewable and Sustainable Energy Reviews*, **105,** 86-94.

TARKOWSKI, R. & CZAPOWSKI, G. (2018) Salt Domes in Poland–Potential Sites for Hydrogen Storage in Caverns. *International Journal of Hydrogen Energy*, **43,** 21414-21427.

TAYLOR, J. (1998) Upper Permian—Zechstein. *Petroleum Geology of the North Sea: Basic concepts and recent advances* (Ed. By Glennie K.W.)**,** 174-211.

URAI, J. & SPIERS, C. (2017) The Effect of Grain Boundary Water on Deformation Mechanisms and Rheology of Rocksalt During Long-Term Deformation. In: *The Mechanical Behavior of Salt–Understanding of Thmc Processes in Salt* (Ed. by, M. Wallner, K. Lux, W. Minkley and H. Hardy Jr.) 149-158. CRC Press.

VAN ADRICHEM BOOGAERT, H. & KOUWE, W. (1993) Stratigraphic Nomenclature of the Netherlands, Revision and Update by Rgd and Nogepa.

VAN GENT, H., URAI, J.L. & DE KEIJZER, M. (2011) The Internal Geometry of Salt Structures–a First Look Using 3d Seismic Data from the Zechstein of the Netherlands. *Journal of Structural Geology*, **33,** 292-311.

WARREN, J.K. (2006) *Evaporites: Sediments, Resources and Hydrocarbons*. Springer Science & Business Media. 1041p.
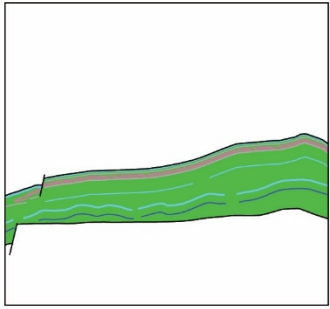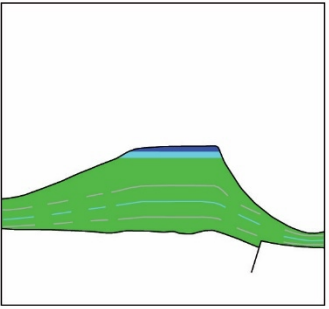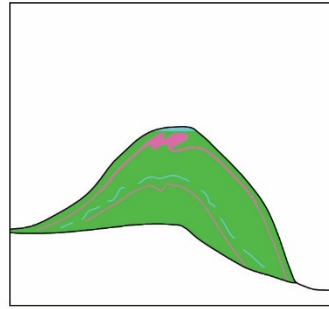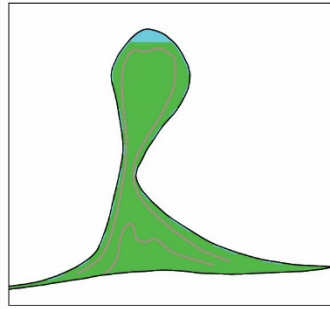
WARREN, J.K. (2018) *Well (wireline) log interpretation of evaporates: An overview.* https://www.saltworkconsultants.com/archive-salty-matters/
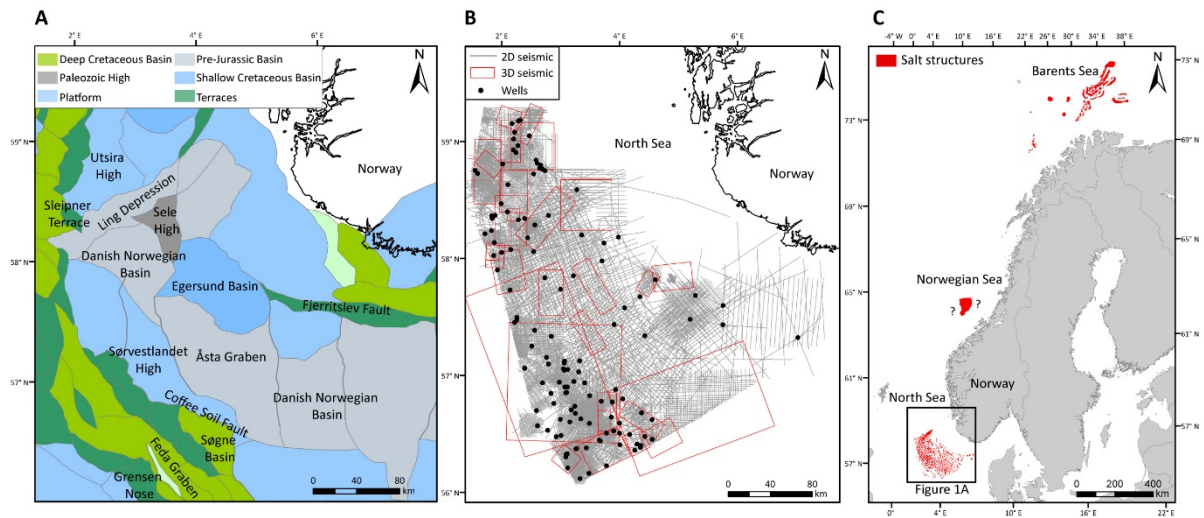
YANG, C., JING, W., DAEMEN, J.J., ZHANG, G. & DU, C. (2013) Analysis of Major Risks Associated with Hydrocarbon Storage Caverns in Bedded Salt Rock. *Reliability Engineering & System Safety*, **113,** 94-111.

**Table 1** Cap rock thickness for some wells in the Norwegian North Sea.

Well	Cap rock thickness (m)	Type of structure
17/4-1	19	weakly deformed salt
17/11-1	17	weakly deformed salt
3/8-1	0	weakly deformed salt
3/5-1	21	weakly deformed salt
17/4-1	19	weakly deformed salt
17/11-1	17	weakly deformed salt
16/7-1	45	Intermediate size salt structure
6/3-2	100	Intermediate size salt structure
7/3-1	43	Intermediate size salt structure
8/10-3	59	Intermediate size salt structure
3/7-2	21	Intermediate size salt structure
8/3-1	80	Flank of a tall diapir
1/6-5	106	Tall diapir

Table 2 Challenges and opportunities for subsurface storage in the different salt structures described in this study. Thin beds are not included due to the lack of halite.

Weakly deformed salt	Intermediate salt structures		Tall diapirs
	K-Mg salt is absent	K-Mg salt is present	
Opportunities	*Opportunities*	*Opportunities*	*Opportunities*
- Halite units of more than 300 m	- Halite units of more than 300 m	- Halite units of more than 300 m	- Halite units of more than 300 m
- Less deformation, higher predictability	- Dendritic geometries provide large areas	- Commonly shallower than 2000 m	- Shallower than 2000 m
- High lateral continuity		- Dendritic geometries provide large areas	- Elongate diapirs have lateral continuity
- Thin cap rock			
- Relatively good seismic image			
Challenges	*Challenges*	*Challenges*	*Challenges*
- Usually deeper than 2000 m	- Usually deeper than 2000 m	- Squezing K-Mg salts and other competent stringers	- High deformation
- Thin stringers of different lithologies, including K-Mg salts	- Thin stringers of competent lithologies	- Thin stringers of different lithologies	- Poor seismic image
	- Cap rock can reach 100 m	- Cap rock can reach 100 m	- Squezing K-Mg salts and other competent stringers
			- Cap rock can reach 100 m
			- Poor lithological control

🟩 Halite 🟦 Anhydrite 🟪 K-Mg salts 🟦 Carbonate ⬜ Claystone

Figure 1 a) Tectonic provinces of the study area (NPD, 2022). b) Subsurface dataset used in this study. c) Regional map of the Norwegian Continental Shelf (NCS) showing the areas where evaporites have been encountered. Salt structures in the Barents Sea are from Rojo and Escalona (2018), Rojo et al. (2019), and Kairanov et al. (2020). The evaporites in the Norwegian Sea, Halten Terrace area, are from Elliot el at. (2021).
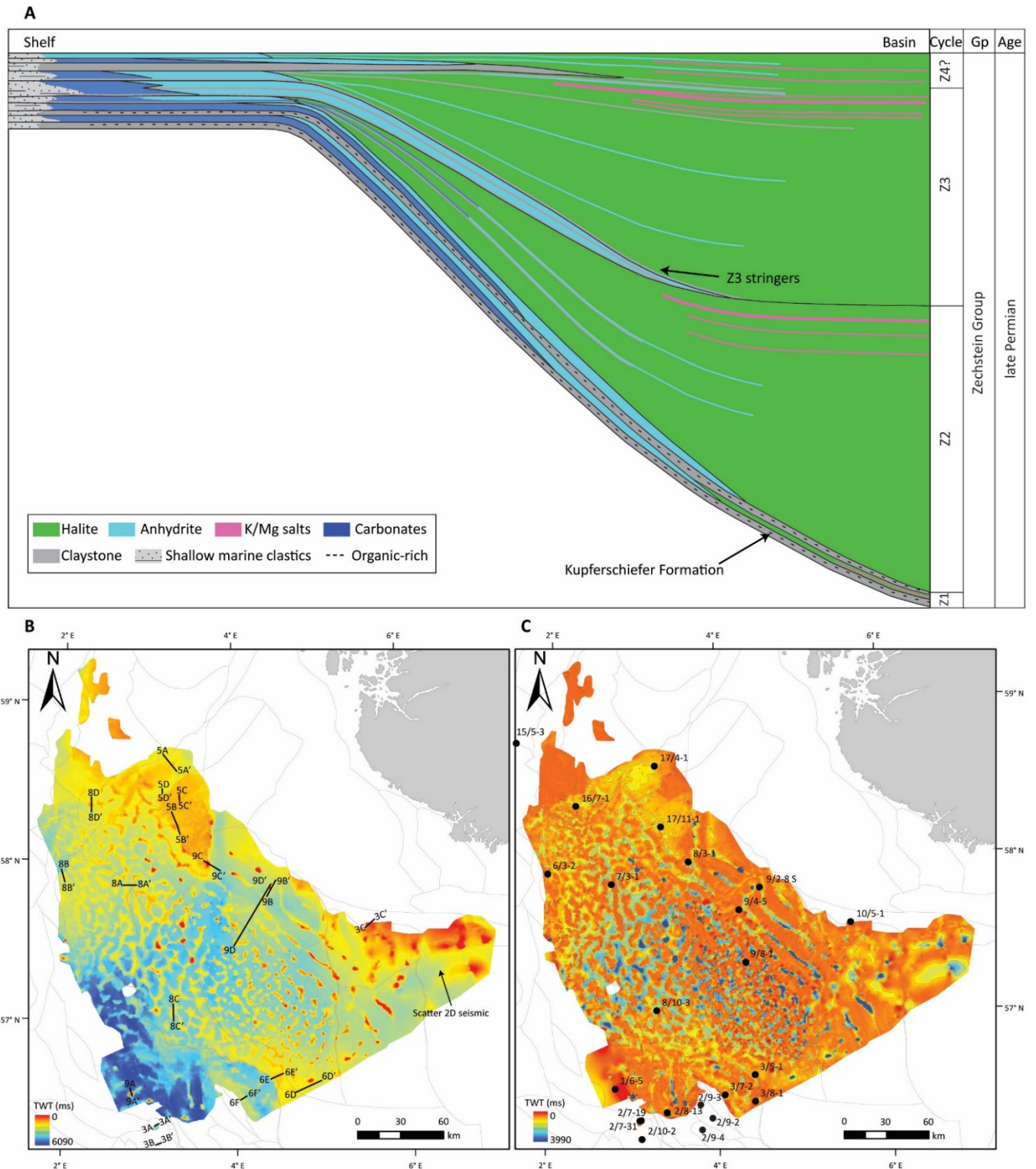
Figure 2 a) Schematic cross section showing the compositional variation of the Zechstein Group in the NNS (adapted from van Adrichem Boogaert and Kouwe, 1993; Clark et al., 1998; Taylor, 1998; Jackson et al., 2019; Pichat, 2022; and the well data of this study). The Zechstein Group cycles (Z1-Z4) are interpreted based on compositional similarities with other North European areas. b) Structure map of the top of the Zechstein Group and location of the seismic lines included in this study. c) Time thickness map of the Zechstein Group and location of the wells used in this study.
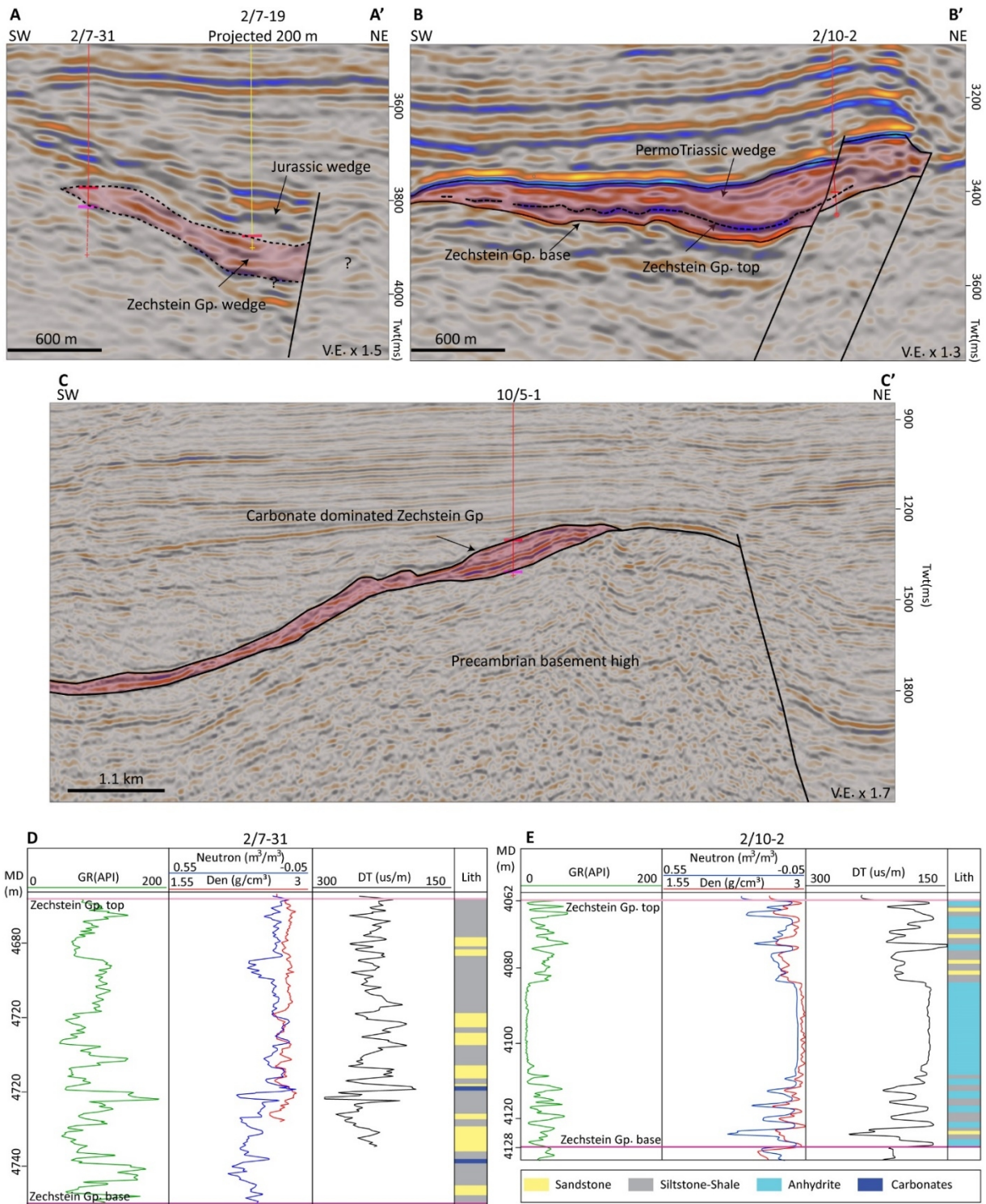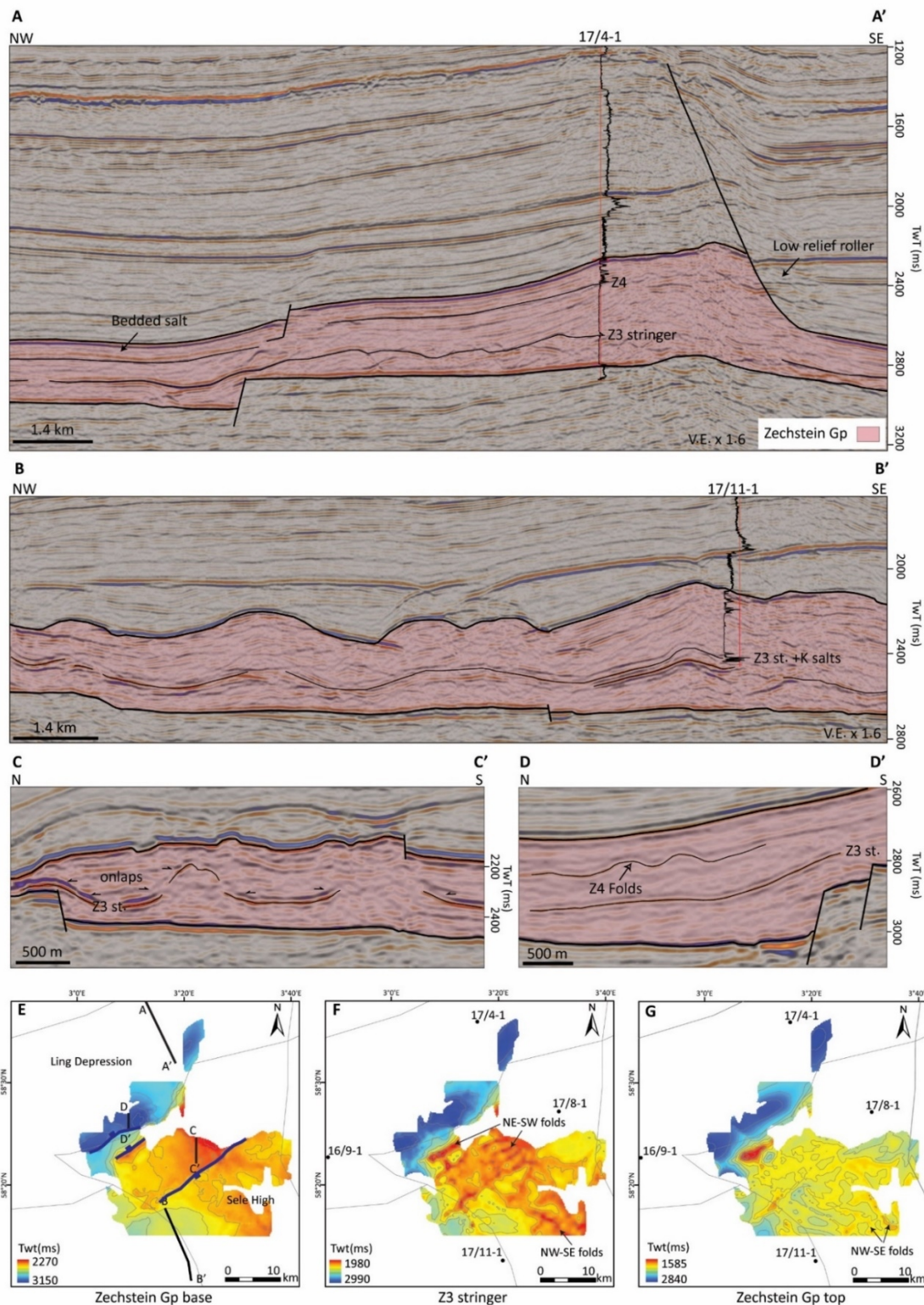
Figure 3 Seismic sections showing a) intra-Zechstein Group growth strata, b) Permo-Triassic growth strata, and c) carbonate dominated Zechstein Group in the Fjerritslev fault zone. Sections A-A' and B-B' from the 3D survey ST99M1-AREA1. Section C-C' from the 2D survey EBS00-121. d) Well 2/7-31 showing a clastic-dominated Zechstein Group. e) Well 2/10-2 showing an anhydrite-claystone dominated Zechstein Group. Location of the seismic sections are in Figure 2b, and those of the wells are in Figure 2c. V.E: vertical exaggeration.
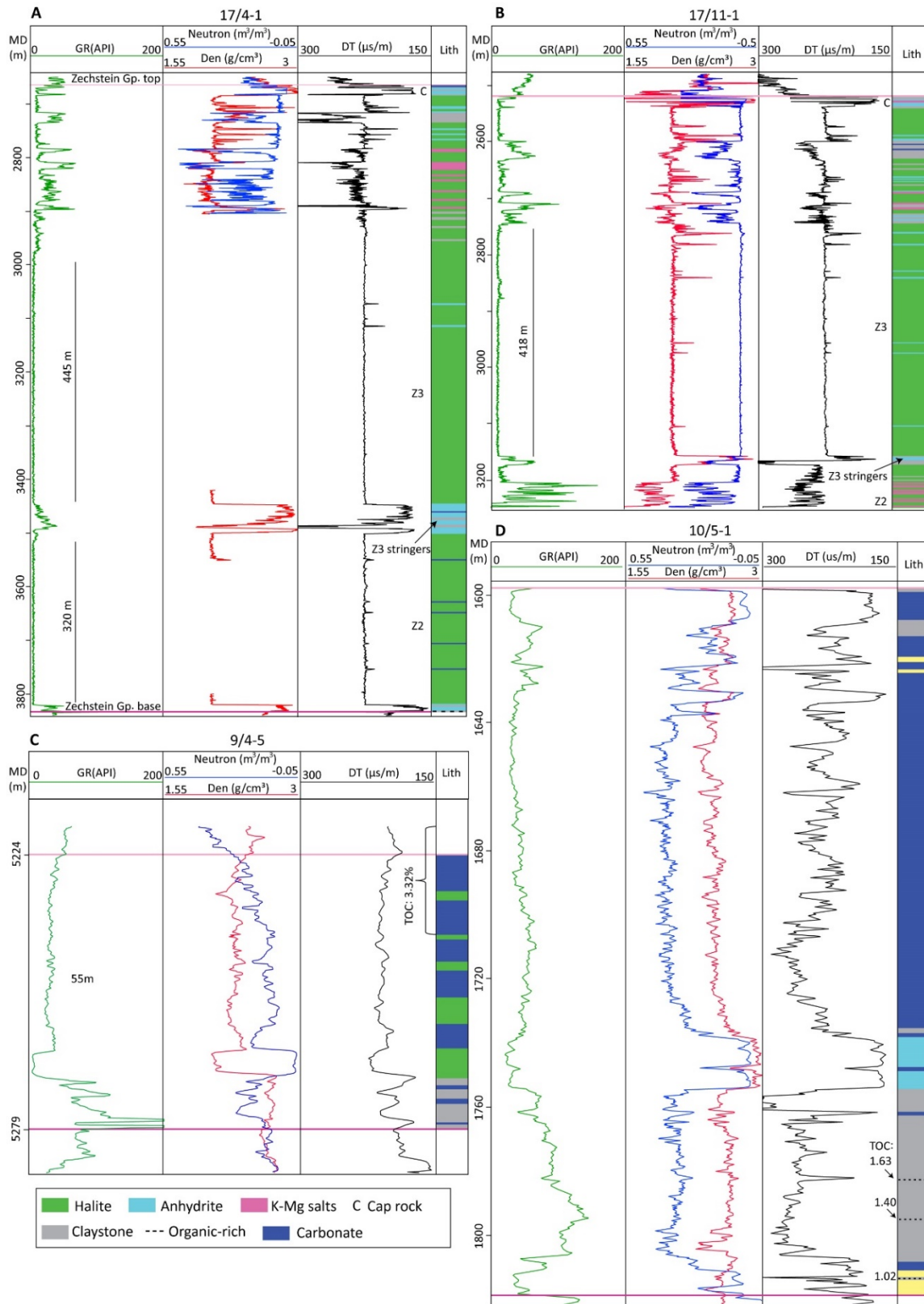
Figure 4 Compositional variation of the Zechstein Group in a) well 17/4-1 in the Ling depression, b) well 17/11-1 close to the Sele High and the NW part of the Danish Norwegian Basin (this well does not reach the base of the Zechstein Group), c) well 9/4-5 in the Egersund Basin (this well penetrates a seismic interpreted salt weld), and d) well 10/5-1 in the Fjerritslev fault zone, TOC values from NPD (2022). Location of the wells are in Figure 2c.

Figure 5 Seismic sections showing the character of the Zechstein Group in a) the Ling depression from the 2D survey GLD-92-205, b) the boundary between the Sele High and the NW Danish Norwegian Basin from the 2D survey GLD-92-204, c) the Sele High from the 3D survey LO1101_MERGE, and d) the boundary between the Ling depression and the Sele High from the 3D survey LO1101_MERGE. Structure maps of e) the Zechstein Group base, f) the Z3 stringer, and g) the Zechstein Group top in the area between wells 17/4-1 and 17-11-1. Location of the seismic sections are in figure 5e. V.E: vertical exaggeration. The Gamma Ray log is displayed for the different wells.
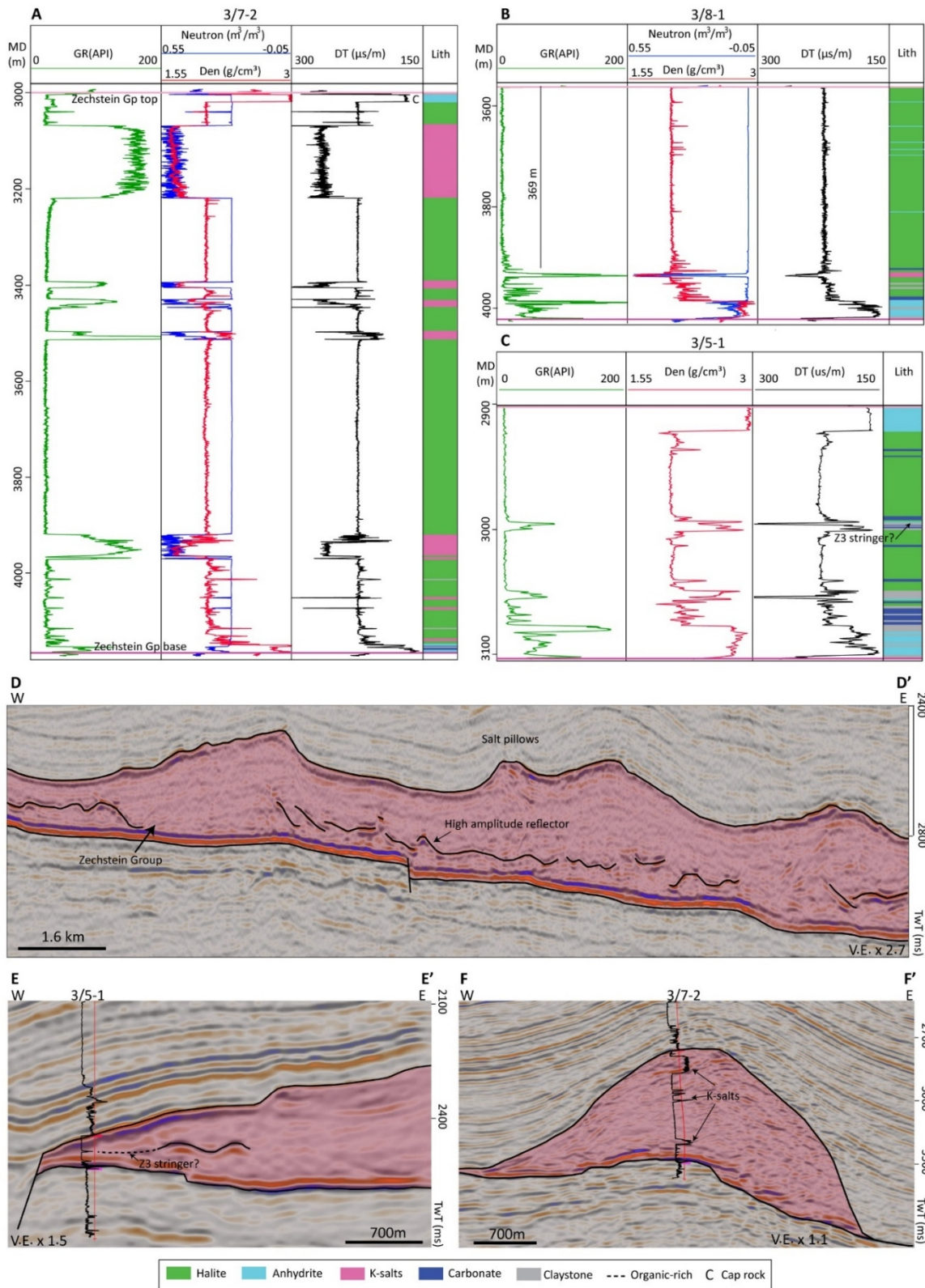
Figure 6 Compositional variation of the Zechstein Group in wells a) 3/7-2 in the Søgne Basin, and b-c) 3/8-1 and 3/5-1 along the Coffee Soil fault complex. Seismic sections d) across the southern Åsta Graben from the 3D survey ST99M1_AREA3, e) along the Coffee Soil fault complex from the 3D survey DNO0601, and f) across the Søgne Basin from the 3D survey SH9003. Location of the seismic sections and wells are in Figures 2b and 2c.
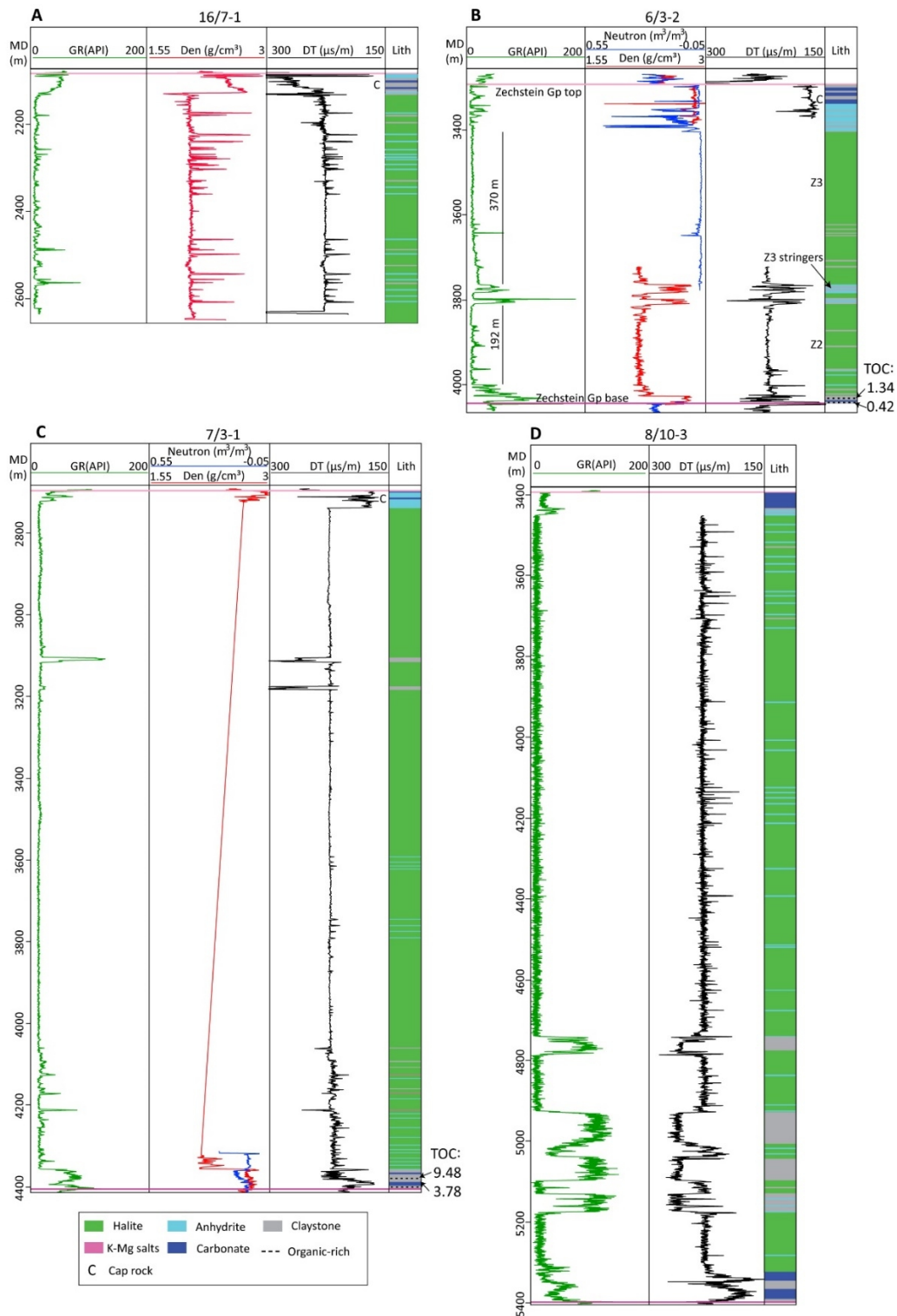
Figure 7 Compositional variation of the Zechstein Group in the intermediate salt structures. a) Well 16/7-1 composed of halite with anhydrite and claystone stringers. b) Well 6/3-2 consisting of two main halite units with anhydrite and claystone stringers. TOC values from NPD (2022). c) Well 7/3-1 displaying a thick sequence of halite with thin stringers of anhydrite, claystone and K-Mg salts. TOC values from Skarstein personal communication, PaBas in-house data. d) Well 8/10-3 consisting of a lower part dominated by carbonate and claystone, followed by halite interbedded with claystone (lower part of the section) and anhydrite stringers (middle to upper part of the section). Location of the wells are in Figure 2c.
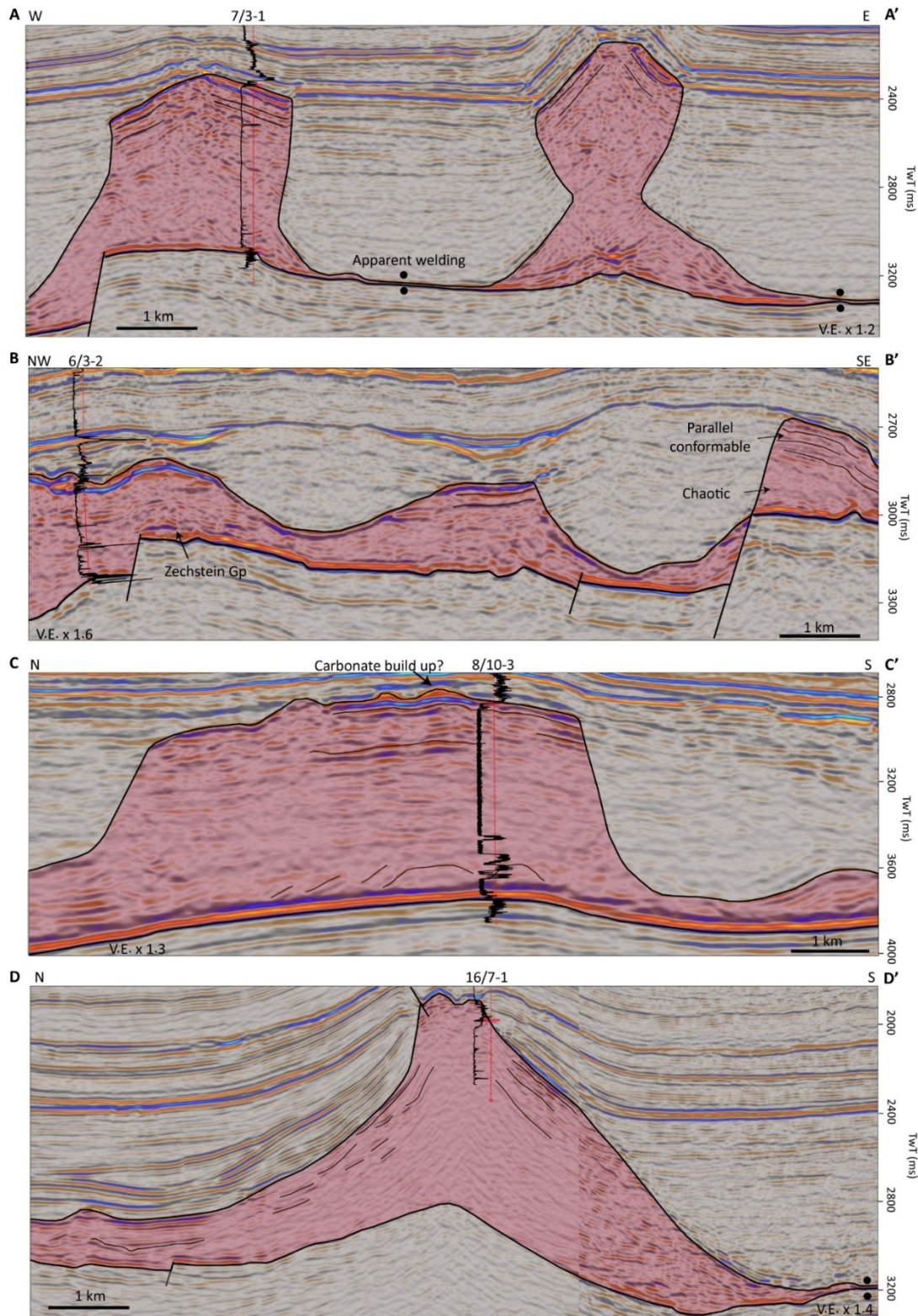
Figure 8 a-d) Seismic sections showing examples of intermediate size salt structures. Location of the seismic sections are in Figure 2b. Section A-A' from the 3D survey ST0710. Section B-B' from the 3D survey NH0201. Section C-C' is courtesy of CGG Services (UK) Limited (Coral survey). Section D-D' from the 3D surveys LN0703, ES9401.
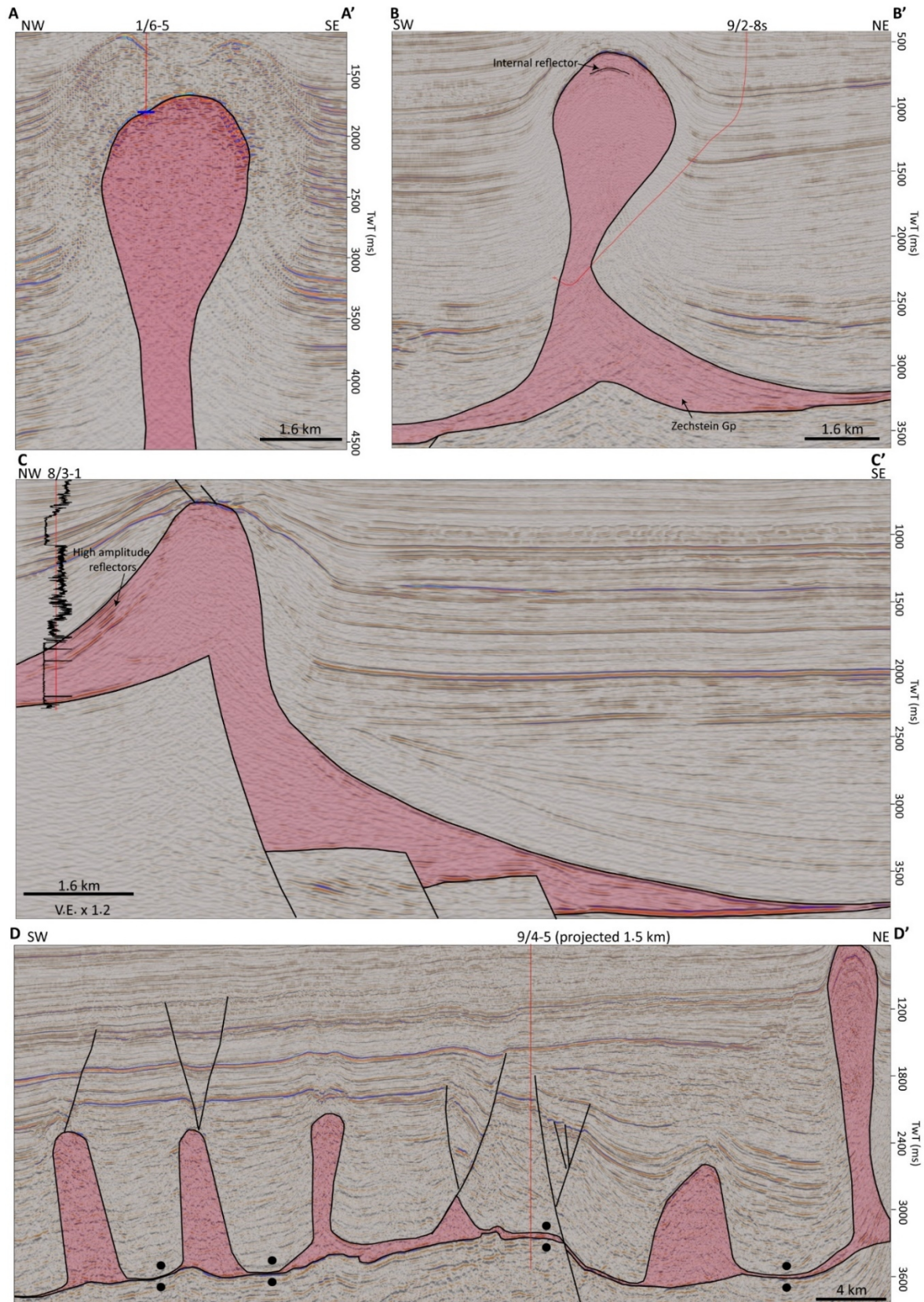
Figure 9 a-d) Seismic sections showing examples of tall diapirs. Location of the seismic sections are in Figure 2b. Section A-A' from the 3D survey ST99M1-AREA1. Section B-B' from the 3D survey ST9413. Section C-C' from the 3D survey MC3D-EGB2008. Section D-D' from the 2D survey UG97-301.
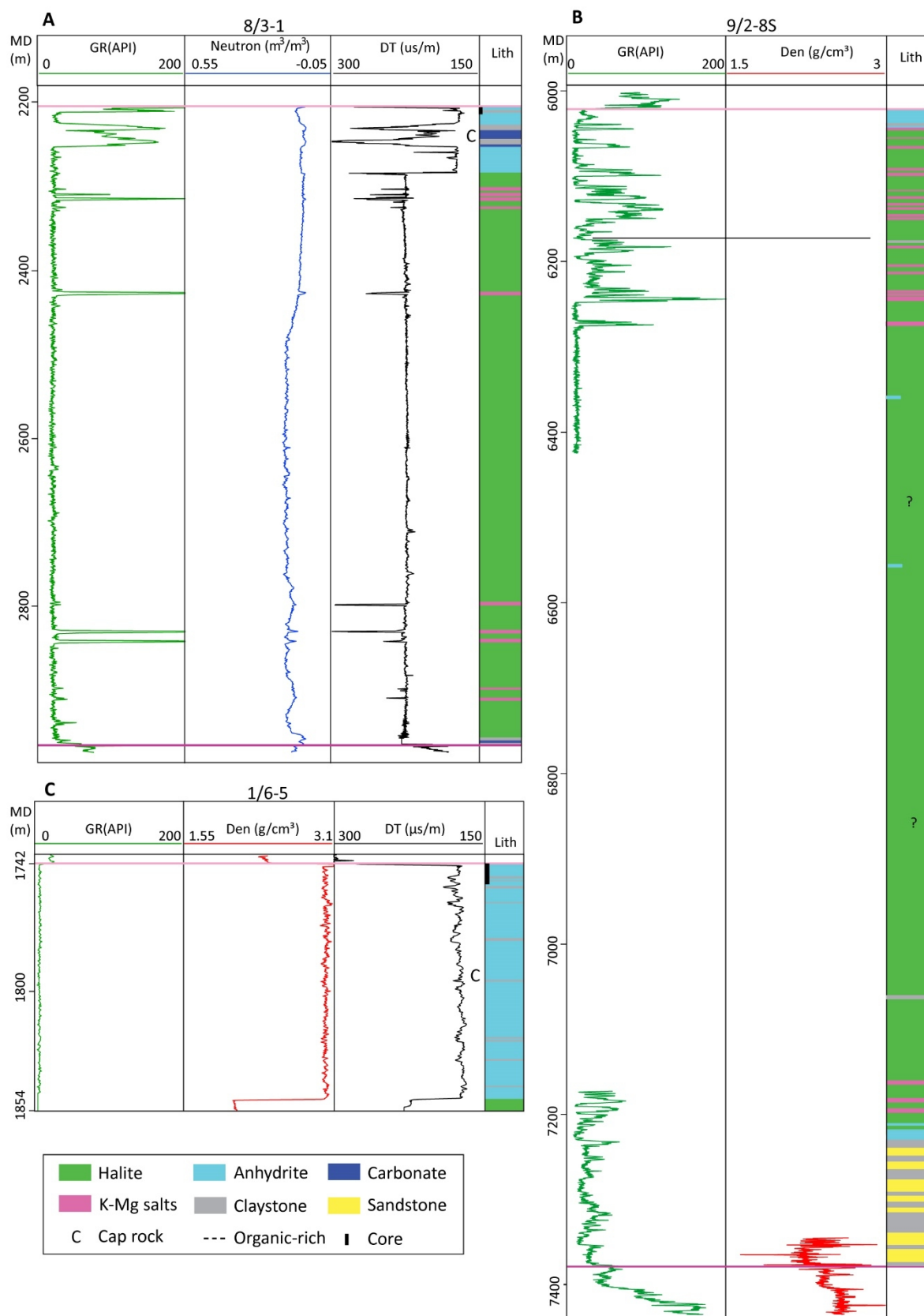
Figure 10 Compositional variation of the Zechstein Group in tall diapirs. a) Well 8/3-1 drilled through the flank of a salt diapir. b) Well 9/2-8s which penetrated the stem of a salt diapir. c) Well 1/6-5 drilled through an anhydrite-dominated cap rock. Location of the wells are in Figure 2c.
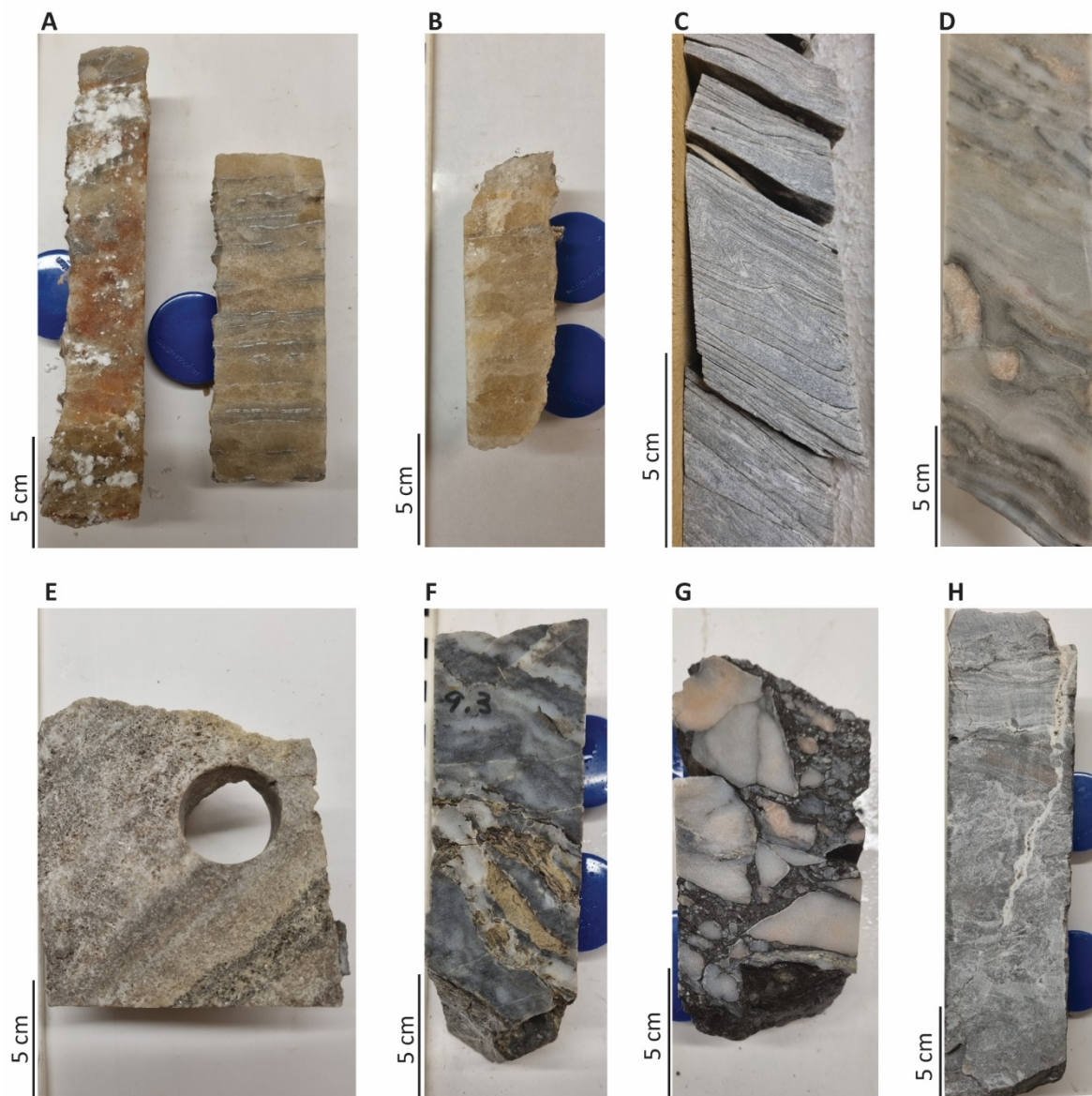
Figure 11 Zechstein Group cores in the Norwegian North Sea. a) Halite with sylvite (left core, NPD2022) and halite with discontinuous stringers of anhydrite and claystone (right core), well 15/5-3. b) Halite, well 15/5-3. c) Folded anhydrite interbedded with thin layers of claystone, well 1/6-5. d) Boudins of competent lithology embedded in anhydrite, well 1/6-5. e) Needle-shaped celestite, well 2/8-13 (NPD, 2022). f) Siltstone stringers within anhydrite, well 8/3-1. g) Breccia, well 9/8-1. h) Sub-vertical vein through a heterolithic cap rock, well 15/12-3. Cores c-h are from cap rock.
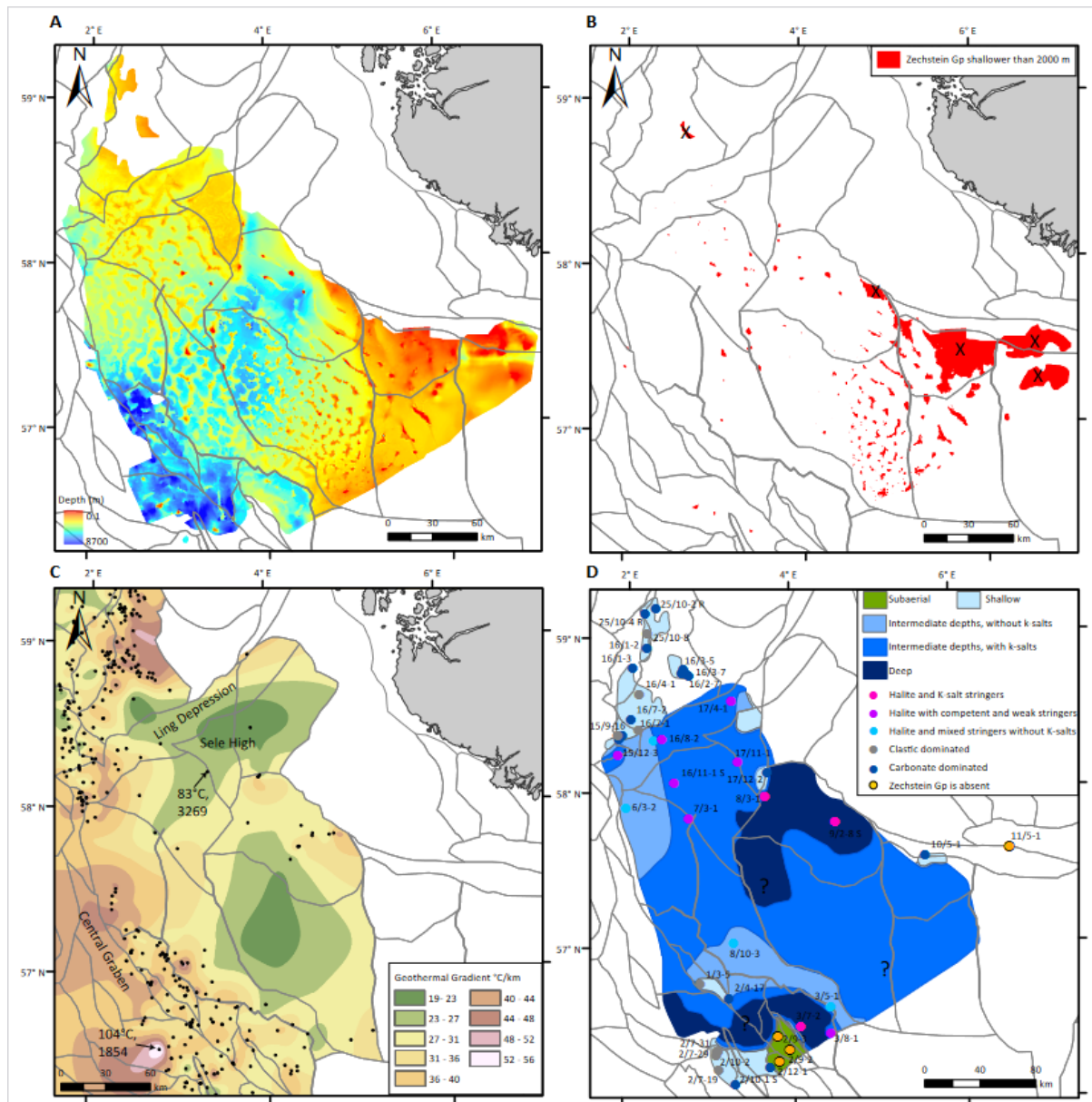
Figure 12 a) Depth map of the Zechstein Group top. b) Map indicating areas where the Zechstein Group is shallower than 2000 m (red polygons). Areas marked with X do not have thick halite layers. c) Geothermal gradient of the study area from the bottom hole temperatures (BHT) of the wells marked with black circles (BHT from NPD, 2022). d) Map showing the interpretation of the paleowater depth for the time of deposition of the Zechstein Group. Shallow areas are carbonate-anhydrite or clastic dominated. Intermediate water depths are dominated by thick halite (see Figure 2c) with mixed stringers. Deep areas are dominated by thick halite, tall diapirs and the most common heterogeneity within the halite are K-Mg salts. This map is modified and expanded from Clark et al. (1998), Sorento et al. (2018), and Jackson et al. (2019). Wells 15/9-16, 16/1-2, 16/3-5, 16/3-7, 16/4-1, 16/7-2, 25/10-4R, and 25/10-2R are from Sorento et al. (2018) and Jackson et al. (2019)

Supplementary material 1 Three-dimensional seismic surveys interpreted in this study

ST9105	MC3D-EGB2008	SST2000
B-88-S	MC3D-EGBEXT2008	ST0203
BPN9102R96	MC3D-Q15	ST0208
CN193	MC3D-Q82008	ST0611
DNO0601	MC3D-VARG2002	ST0710
ES9401	NH0201	ST8802
ES9402	NH0504	ST9413
G-9603	NH9301R97	ST9702M
GA3D93	Coral (CGG)	ST98M2
LN0703	PN9401M	ST98M3
LN10M08_B	SG9508M	ST99M1-AREA1
LO1101_MERGE	SG9703	ST99M1-AREA3
MC3D-EGB2005	SH9003	UP96

Supplementary material 2 Two-dimensional seismic surveys interpreted in this study

GFR-93	SET96	ST8626R90
FB-92	NDBRE96	SHDE98
ST8629	GUGM-94	SHDEI98
SKAGRE96	GNSR-91	GLD-92
MN9206	ST8713	81M-03
EBS00	ST8606	ST8107WE
ST8712	PSL84	BPN88
SG8726	NDBE96	ST9216
ST8606	ST8716	ST8603R92
UGI98	ST8716R91	ST8108R94
ST8605	SH8709R91	ST8315
SHD97	ANO78	HPS98
UG97	CAST-90	ST8107GE
MN9604	SG9706	SE93

Supplementary material 3 Wells that penetrate the Zechstein Group (NPD, 2022)

1/3-1	2/7-19	7/12-3 A	16/1-16
1/3-3	2/7-19 R	7/12-5	16/1-29 S
1/3-4	2/7-28	8/1-1	16/2-6
1/3-5	2/7-29	8/3-1	16/2-7
1/5-2	2/7-31	8/4-1	16/2-16
1/5-4 S	2/8-7	8/9-1	16/3-5
1/6-1	2/8-13	8/10-1	16/3-7
1/6-5	2/8-17 A	8/10-2	16/3-8 A
1/9-4	2/9-5 S	8/10-3	16/3-8 S
1/9-4 R	2/10-1 S	8/10-4 S	16/4-1
2/1-2	2/10-2	8/10-5 A	16/5-3
2/1-3	2/11-12 A	8/10-5 S	16/7-1
2/1-4	2/12-1	8/10-6 S	16/7-2
2/1-7	3/4-1	8/10-7 S	16/7-3
2/1-9	3/5-1	9/2-8 S	16/8-2
2/2-1	3/7-2	9/4-1	16/8-3 S
2/2-2	3/7-3	9/4-5	16/9-1
2/2-5	3/7-4	9/8-1	16/10-1
2/3-1	3/7-5	10/4-1	16/10-4
2/3-3	3/7-8 S	10/5-1	16/11-1 S
2/3-4	3/7-11 S	10/7-1	16/11-2
2/4-8	3/8-1	10/8-1	17/4-1
2/4-11	6/3-2	11/9-1	17/11-1
2/4-17	7/3-1	15/2-1	17/12-1 R
2/4-20	7/4-1	15/5-3	17/12-2
2/4-22 S	7/4-2	15/9-9	25/10-2 R
2/5-3	7/7-2	15/9-13	25/10-4
2/6-1	7/7-3	15/9-16	25/10-4 R
2/6-2	7/8-2	15/12-2	25/10-8
2/6-3	7/8-3	15/12-3	25/10-10
2/6-4 S	7/9-1	15/12-17 S	25/10-15 S
2/6-6 S	7/11-1	15/12-18 S	25/11-17
2/7-3	7/11-7	16/1-2	
2/7-12	7/11-7 R	16/1-3	

Supplementary material 4 Wells with bottom hole temperatures used to create the geothermal gradient map of Fig. 12c (NPD, 2022)

1/2-2	15/12-3	15/9-18	16/2-22 S	2/11-3 A
1/3-10	15/12-4	15/9-19 A	16/2-3	2/1-13 S
1/3-10 A	15/12-5	15/9-19 B	16/2-4	2/11-5
1/3-11	15/12-6 S	15/9-22	16/2-5	2/1-15
1/3-3	15/12-7 S	15/9-4	16/2-7	2/11-6 S
1/3-4	15/12-8	15/9-5	16/2-8	2/11-7
1/3-5	15/12-8 A	15/9-6	16/2-9 S	2/12-1
1/3-6	15/12-9 S	15/9-7	16/3-4	2/12-2 S
1/3-7	15/3-2 R	15/9-8	16/3-5	2/1-3
1/3-8	15/3-3	16/10-1	16/3-7	2/1-4
1/3-9 S	15/3-5	16/10-2	16/3-8 S	2/1-5
1/5-3 S	15/3-7	16/10-3	16/4-1	2/1-6
1/5-4 S	15/3-8	16/10-4	16/4-2	2/1-7
1/5-5	15/3-9	16/1-10	16/4-4	2/1-8
1/6-5	15/5-3	16/1-11	16/4-5	2/1-9
1/6-6	15/5-4	16/11-1 S	16/4-6 S	2/1-9 A
1/6-7	15/5-5	16/1-12	16/4-7	2/2-1
1/9-3	15/5-6	16/1-13	16/4-9 S	2/2-2
1/9-6 S	15/6-1	16/1-14	16/5-1	2/2-3
1/9-6 SR	15/6-10	16/1-15	16/6-1	2/2-4
1/9-7	15/6-11 A	16/1-17	16/7-1	2/2-5
11/10-1	15/6-12	16/1-21 S	16/7-2	2/3-3
15/12-1	15/6-13	16/1-22 A	16/7-3	2/3-4
15/12-10 S	15/6-2 R	16/1-22 S	16/7-4	2/4-13
15/12-11 S	15/6-4	16/1-27	16/7-6	2/4-14
15/12-12	15/6-6	16/1-3	16/7-7 S	2/4-15 S
15/12-13	15/6-7	16/1-5	16/7-8 S	2/4-16
15/12-13 A	15/6-8 A	16/1-6 S	16/7-9	2/4-17
15/12-13 B	15/6-8 S	16/1-7	16/8-2	2/4-18 R
15/12-14	15/6-9 A	16/1-8	16/8-3 S	2/4-20
15/12-15	15/6-9 B	16/1-9	16/9-1	2/4-21
15/12-16 S	15/6-9 S	16/2-1	17/11-1	2/4-22 S
15/12-17 A	15/8-1	16/2-10	17/12-1 R	2/4-23 S
15/12-17 S	15/8-2	16/2-11	17/12-4 A	2/4-4
15/12-18 A	15/9-1	16/2-12	17/12-4 B	2/4-6
15/12-18 S	15/9-10	16/2-14	17/3-1	2/5-10
15/12-19	15/9-12	16/2-15	17/9-1 R	2/5-10 A
15/12-2	15/9-12 R	16/2-17 S	2/10-2	2/5-11
15/12-20 S	15/9-13	16/2-18 S	2/1-10	2/5-12
15/12-21	15/9-14	16/2-19	2/1-11	2/5-13
15/12-21 A	15/9-15	16/2-2	2/11-10 S	2/5-7
15/12-23	15/9-16	16/2-20 S	2/1-12	2/5-8

2/5-9	2/8-7	25/11-18	3/7-4	7/12-7 R
2/6-3	2/9-3	25/11-20	3/7-6	7/12-8
2/6-4 S	2/9-4	25/11-21 A	3/7-7	7/12-9
2/6-5	24/12-1	25/11-21 S	3/7-8 S	7/3-1
2/7-13	24/12-1 R	25/11-22	3/7-9 S	7/4-2
2/7-15	24/12-2	25/11-24	4/4-1	7/7-1
2/7-16	24/12-3 S	25/11-25 A	6/3-1	7/7-2
2/7-17	24/12-4	25/11-25 S	6/3-2	7/7-3
2/7-19	24/12-5 S	25/11-27	7/11-10 S	7/7-4
2/7-19 R	24/9-3	25/11-28	7/11-10 SR	7/8-3
2/7-20	25/10-1	25/11-9	7/11-11 S	7/8-4
2/7-21 S	25/10-1 R	25/7-1 S	7/11-12 S	7/8-5 S
2/7-22	25/10-13 S	25/7-2	7/11-5	8/10-2
2/7-23 S	25/10-2 R	25/7-4 S	7/11-6	8/10-3
2/7-24	25/10-3	25/8-10 S	7/11-7	8/10-4 S
2/7-26 S	25/10-4	25/8-11	7/11-7 R	8/10-5 S
2/7-27 S	25/10-4 R	25/8-12 A	7/11-8	8/10-6 S
2/7-28	25/10-6 S	25/8-12 S	7/11-9	8/3-2
2/7-29	25/10-7 S	25/8-14 S	7/1-2 S	8/4-1
2/7-30	25/10-9	25/8-15 S	7/12-10	9/2-1
2/7-31	25/11-10	25/8-18 S	7/12-11	9/2-2
2/8-10	25/11-11	25/8-4	7/12-12 S	9/2-3
2/8-12 S	25/11-12	3/4-1	7/12-13 S	9/2-4 S
2/8-13	25/11-13	3/4-2 S	7/12-3 A	9/2-5
2/8-15	25/11-14 S	3/5-1	7/12-4	9/3-1
2/8-17 A	25/11-15	3/5-2	7/12-5	9/3-2
2/8-17 S	25/11-16	3/6-1	7/12-6	9/4-5
2/8-2	25/11-17	3/7-2	7/12-7	